Lecture 4

Correlation effects in hopping conductivity

Topics:

1. *Coulomb gap and multielectron hops*
2. *Correlated transport via a two-site chain*
3. *Coulomb drag in hopping transport*
4. *Spin correlations in organic magnetoresistance*

Coulomb gap

random on-site energies

$$H = \sum \phi_i n_i + \frac{1}{2} \sum_{i \neq j} \left(n_i - \tfrac{1}{2}\right)\left(n_j - \tfrac{1}{2}\right) e_{ij}$$

$$e_{ij} = e^2/\kappa r_{ij}$$

$$P(\phi) = \begin{cases} (2A)^{-1}, & |\phi| < A, \\ 0, & |\phi| > A. \end{cases}$$

$n_i = 1$ if the site is occupied and $n_i = 0$ if it is empty

The energy of site i $\quad \epsilon_i = \phi_i + \sum_j e_{ij}\left(n_j - \tfrac{1}{2}\right)$

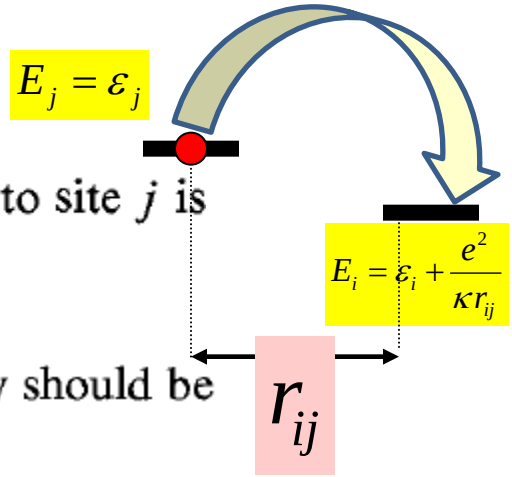

The change of the total energy upon moving the electron from site i to site j is

$$\Omega_i^j = \epsilon_j - \epsilon_i - e^2/\kappa r_{ij}$$

From the ground state of the system all the changes of the energy should be positive. So the inequality

$\epsilon_j - \epsilon_i - e^2/\kappa r_{ij} \geq 0$ has to be valid for all occupied sites i and all empty sites j in the system.

sites with energies close to the Fermi level are far from each other ⇨ $N(\varepsilon) \sim \left[\frac{\kappa |\varepsilon - \mu|}{e^2}\right]^D$

3D $\quad g(\epsilon) = \mathrm{d}N/\mathrm{d}\epsilon = \alpha_3 (\epsilon - \mu)^2 \kappa^3 / e^6$

2D $\quad g(\epsilon) = \alpha_2 |\epsilon - \mu| \kappa^2 / e^4$

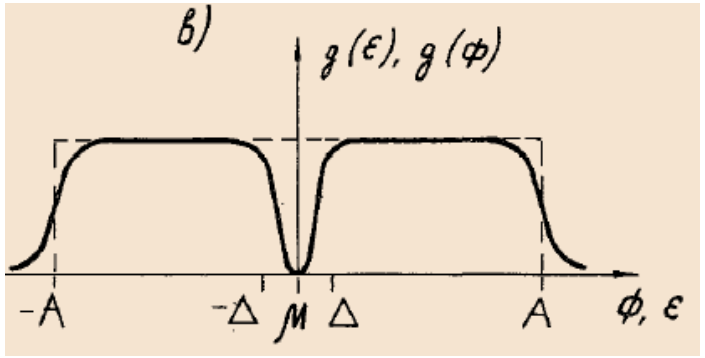

PHYSICAL REVIEW B VOLUME 56, NUMBER 3 15 JULY 1997-I

Screening of the Coulomb interaction in two-dimensional variable-range hopping

F. W. Van Keuls* and X. L. Hu†
Department of Physics, Case Western Reserve University, Cleveland, Ohio 44106

H. W. Jiang
Department of Physics, University of California at Los Angeles, Los Angeles, California 90024

A. J. Dahm
Department of Physics, Case Western Reserve University, Cleveland, Ohio 44106

(Received 6 July 1995; revised manuscript received 12 December 1996)

A Coulomb gap in the density of states is inferred from variable-range-hopping measurements in two dimensions in a gated GaAs/$Al_xGa_{1-x}As$ heterostructure. For large hopping lengths the Coulomb interaction is screened by a metallic gate, and a universal crossover to Mott hopping at low temperatures is observed. Excellent agreement with theory is achieved by adjusting a single combination of constants associated with variable-range hopping. This change in constants is explained by correlated hopping. The Coulomb interaction is not screened by the two-dimensional electron layer. [S0163-1829(97)06927-0]

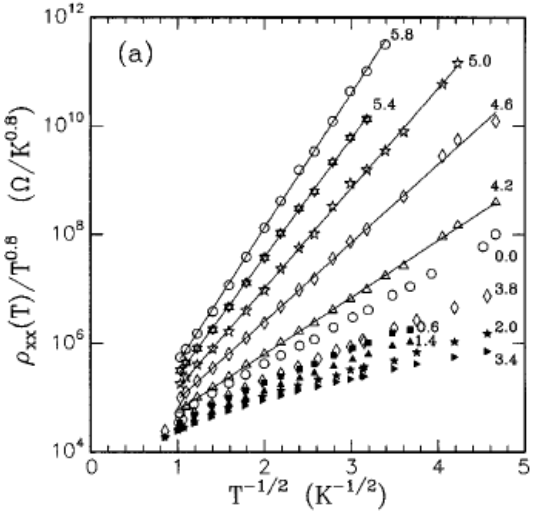

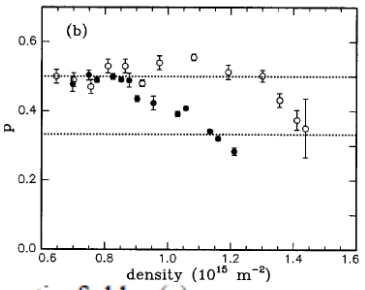

FIG. 2. The ratio $\rho_{xx}/T^{0.8}$ at various magnetic fields, (a) vs $T^{-1/2}$ and (b) vs $T^{-1/3}$. Data are taken on sample A at a density of 1.36×10^{15} m^{-2}. Curves are labeled with the value of B in T.

We determine the temperature dependence of the prefactors empirically in the following manner. We assume the prefactor to be of the form AT^m, and fit our data to

$$\rho_{xx}=A_iT^m\exp(T_i/T)^p, \quad (8)$$

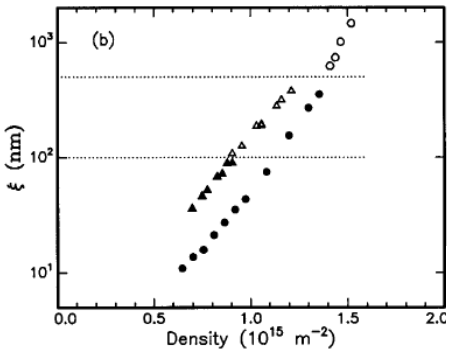

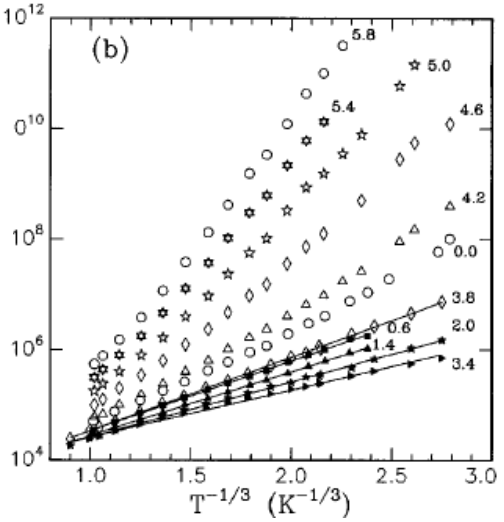

FIG. 6. Localization lengths along two cuts in the n-B plane with the constant $C=1.4$. △—$d=90$ nm; ○—$d=320$ nm. (a) ξ vs B: $n=1.13\times10^{15}$ m^{-2} for $d=90$ nm; $n=1.36\times10^{15}$ m^{-2} for $d=320$ nm. The dashed line represents the cyclotron radius. (b) ξ vs n for $B=0$. Closed and open symbols are taken from the CES and CSM hopping regimes, respectively. Dotted lines indicate approximate values of ξ which separate regimes for the temperature ranges used in this experiment.

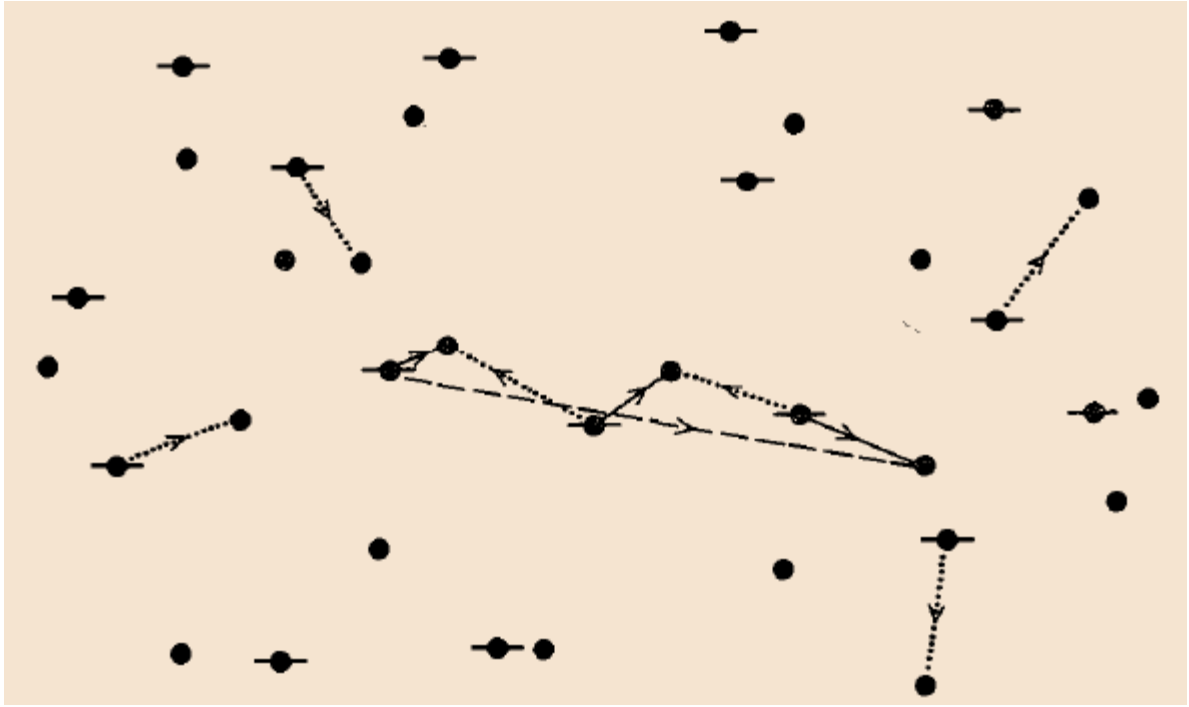

Fig. 8. An example of a many-electron hopping transition, showing a long hop (dashed line), and several shorter hops (dotted lines). In this form the transition is a "polaron" transition. The long and two of the short hops can be replaced by three other short hops (solid lines). These, together with the four remaining short hops, constitute the cascade version of this transition.

While it is generally agreed that many-electron hopping can alleviate the obstacle which the Coulomb gap presents to dc transport at low temperature, some aspects of many-electron hopping have been controversial.

PHYSICAL REVIEW B **74**, 035117 (2006)

Regimes of correlated hopping via a two-site interacting chain

E. I. Levin, V. L. Nguen, and B. I. Shklovskii, Sov. Phys. JETP **55**, 921 (1982)

K. S. Chase and D. J. Thouless, Phys. Rev. B **39**, 9809 (1989)

Y. A. Kinkhabwala and A. N. Korotkov, Phys. Rev. B **62**, R7727 (2000)

Nonohmic hopping transport at $T = 0$

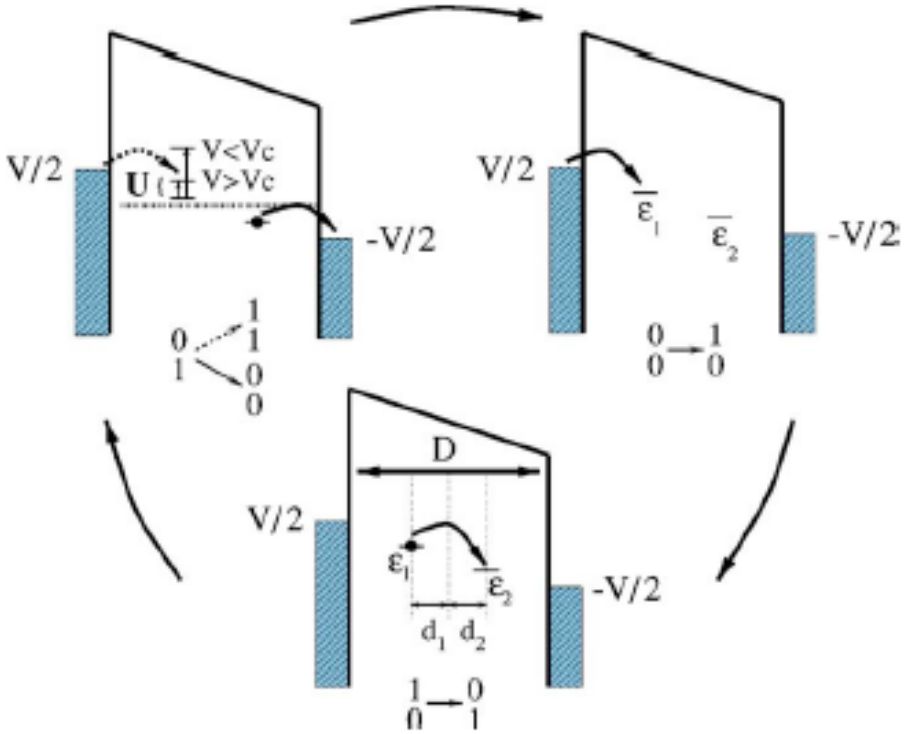

The moments of hops $l \to 1$,

$1 \to 2$ *and* $2 \to r$ *are*

correlated *due to:*

1. *On-site Hubbard repulsion* ⇨ *hops occur only between singly-occupied and empty sites*

2. *Inter-site Coulomb interaction: when the site* 2 *is occupied, the energy of the site* 1 *is shifted up by* U *"charging" energy*

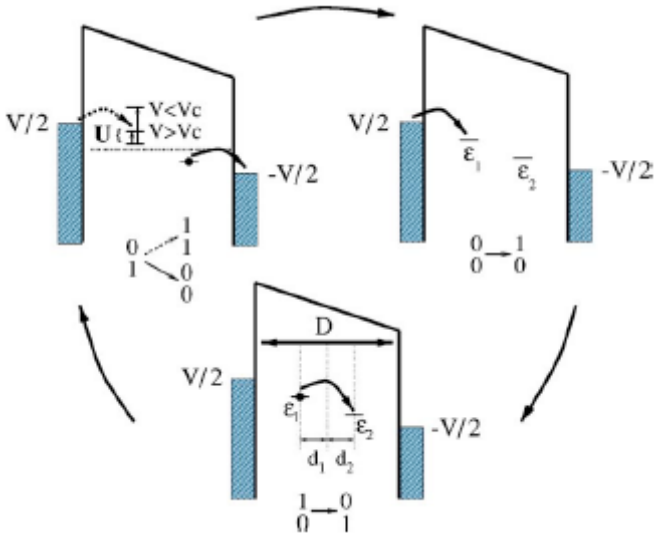

Occupations of sites evolve with time as $0 \to 1 \to 0....$

Within Miller-Abrahams description

$n(t)$ *is replaced by* $< n >$

ε_1 *is the energy of the site* 1 *when the site* 2 *is empty*

ε_2 *is the energy of the site* 2 *when the site* 1 *is empty*

Waiting time for the hop $l \to 1$

$$\tau_1^{-1} = \frac{1}{\hbar} f_l(\varepsilon_1)\Gamma_l(\varepsilon_1)$$

Fermi distribution in the lead *Tunnel width of the level* ε_1

$$\Gamma_l(\varepsilon) = 2\pi \sum_{\mathbf{k}} |t_{1,k}|^2 \delta(\varepsilon - \varepsilon_{\mathbf{k}}) \propto \exp\left[-\frac{D-2d_1}{a}\right]$$

Waiting time for the hop $2 \to r$

$$\tau_3^{-1} = \frac{1}{\hbar}[1 - f_r(\varepsilon_2)]\Gamma_r(\varepsilon_2)$$

$$\Gamma_r(\varepsilon) = 2\pi \sum_{\mathbf{p}} |t_{2,p}|^2 \delta(\varepsilon - \varepsilon_{\mathbf{p}}) \propto \exp\left[-\frac{D-2d_2}{a}\right]$$

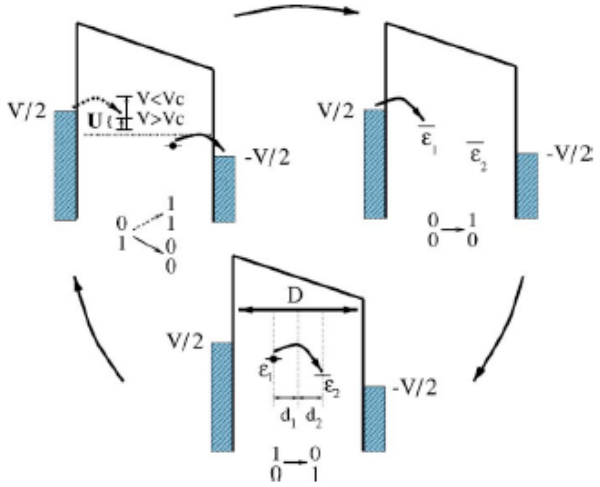

Waiting time for the hop $1 \to 2$

$$\tau_2 \propto \exp\left[\frac{2(d_1+d_2)}{a}\right]$$

At large bias the current path consists of the hops $l \to 1$, $1 \to 2$ *and* $2 \to r$

in ***arbitrary*** *order, i.e. waiting time for* $l \to 1$ *does not depend on the occupation of* 2

Mean-field description

$$\frac{d<n_1>}{dt} = \frac{1-<n_1>}{\tau_1} - \frac{<n_1>(1-<n_2>)}{\tau_2} = 0$$

$$\frac{d<n_2>}{dt} = \frac{<n_1>(1-<n_2>)}{\tau_2} - \frac{<n_2>}{\tau_3} = 0$$

$$I_2^{MF} = \frac{e<n_2>}{\tau_3} = \frac{2e}{\tau_1+\tau_2+\tau_3+[(\tau_1+\tau_2+\tau_3)^2-4\tau_1\tau_3]^{1/2}}$$

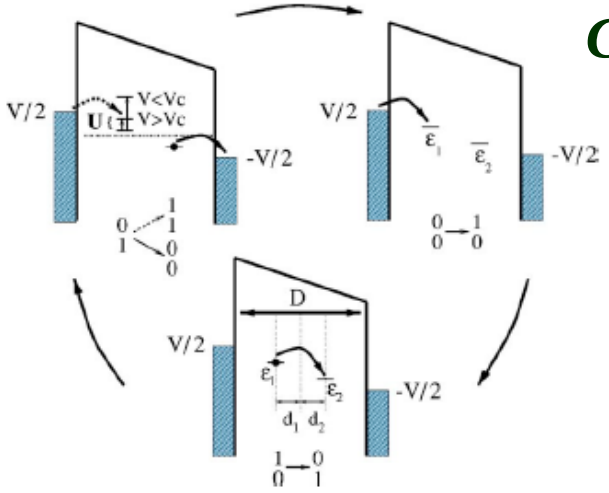

Charging effect impedes hopping transport at

$V < V_c$ ***where*** $\varepsilon_1 + U = \frac{V_c}{2}$

$l \to 1$ ***is possible only if site*** 2 ***is empty***

$$\frac{d < n_1 >}{dt} = \frac{(1 - < n_2 >)(1 - < n_1 >)}{\tau_1} - \frac{< n_1 > (1 - < n_2 >)}{\tau_2} = 0$$

$$\frac{d < n_2 >}{dt} = \frac{< n_1 > (1 - < n_2 >)}{\tau_2} - \frac{< n_2 >}{\tau_3} = 0$$

$$I_1^{MF} = \frac{e}{\tau_1 + \tau_2 + \tau_3}$$

Current step from I_1^{MF} ***to*** I_2^{MF} ***at*** $V = V_c$

Rigorous description

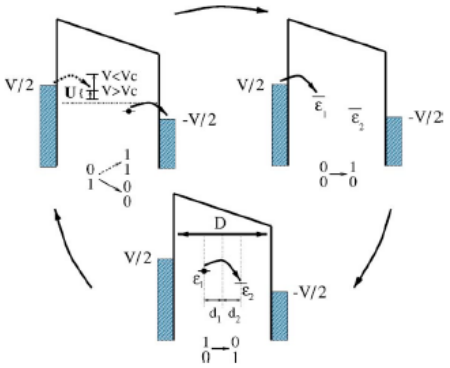

Four possible sets of occupation numbers of the sites

$$(n_1, n_2) = (0,0),\ (1,0),\ (0,1),\ (1,1)$$

$$\frac{dP_{1,0}}{dt} = -\frac{P_{1,0}}{\tau_2} + \frac{P_{0,0}}{\tau_1} + \frac{P_{1,1}}{\tau_3}\Theta(V - V_c)$$

$$\frac{dP_{0,1}}{dt} = -\frac{P_{0,1}}{\tau_3} - \frac{P_{0,1}}{\tau_1}\Theta(V - V_c) + \frac{P_{1,0}}{\tau_2}$$

$$\frac{dP_{0,0}}{dt} = -\frac{P_{0,0}}{\tau_1} + \frac{P_{0,1}}{\tau_3}$$

$$P_{0,0} + P_{0,1} + P_{1,0} + P_{1,1} = 1$$

$$I = \frac{eP_{0,1}}{\tau_3} + \frac{eP_{1,1}}{\tau_3}\Theta(V - V_c)$$

$$I_1 = \frac{e}{\tau_1 + \tau_2 + \tau_3} = I_1^{MF}$$

$$(0,0) \rightarrow (1,0) \rightarrow (0,1) \rightarrow (0,0)$$

$$I_2 = \frac{e(\tau_1 + \tau_3)}{\tau_1^2 + \tau_3^2 + \tau_1\tau_3 + \tau_1\tau_2 + \tau_2\tau_3} < I_2^{MF}$$

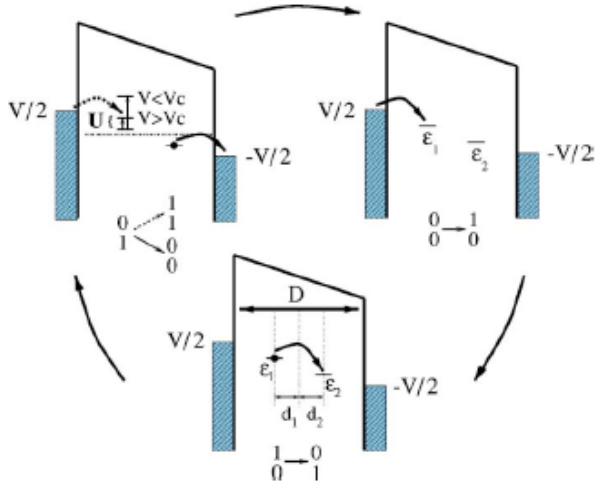

Finite U *allows two-electron hop*

$l \to 1$

$2 \to r$

which facilitates the transport

Waiting time for two-electron hop

$$\frac{1}{\tau_c} = \frac{2\pi}{\hbar}\sum_{k,p} |t_{1,k}t_{2,p}|^2 \left[\frac{1}{\varepsilon_2 - \varepsilon_p} + \frac{1}{\varepsilon_k - \varepsilon_1 - U}\right]^2 \delta(\varepsilon_k + \varepsilon_2 - \varepsilon_p - \varepsilon_1) f_l(\varepsilon_k)[1 - f_r(\varepsilon_p)]$$

vanishes for $U = 0$ *(cotunneling)*

possible for

$$\varepsilon_1 - V/2 < \varepsilon_2 + V/2$$

$$\tau_2 \propto \exp\left[\frac{2(D - d_1 - d_2)}{a}\right]$$

Two-electron hop is equivalent to transfer $l \to r$ *followed by* $2 \to 1$

For $U >> \varepsilon_1 - \frac{V}{2}, \varepsilon_2 + \frac{V}{2}$

$$\frac{1}{\tau_c} = \left(\frac{2\Gamma_l\Gamma_r}{\pi\hbar}\right)\frac{\varepsilon_2 - \varepsilon_1 + V}{(2\varepsilon_1 - V)(2\varepsilon_2 + V)}$$

Can two-electron hops dominate the transport?

Current cycle

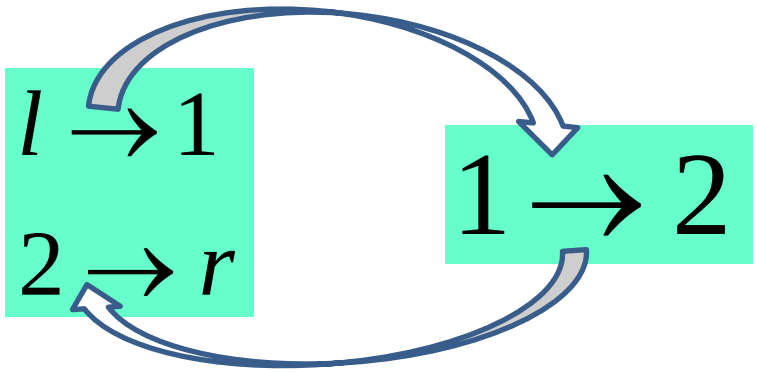

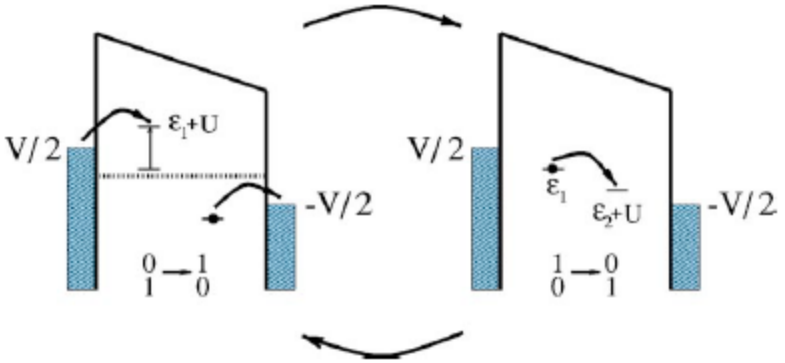

Condition for two-electron hop: $V > (\varepsilon_1 - \varepsilon_2)$.

Current magnitude $I_c = \dfrac{e}{\tau_2 + \tau_c}$

Conditions that $l \to 1$ $2 \to r$ *are blocked*

$(\varepsilon_1 + U) > V/2$ $\varepsilon_2 < -V/2$,

Conditions that two-electron hop is followed by $1 \to 2$

$\varepsilon_2 + U > -\dfrac{V}{2}$ $\varepsilon_1 < \dfrac{V}{2}$

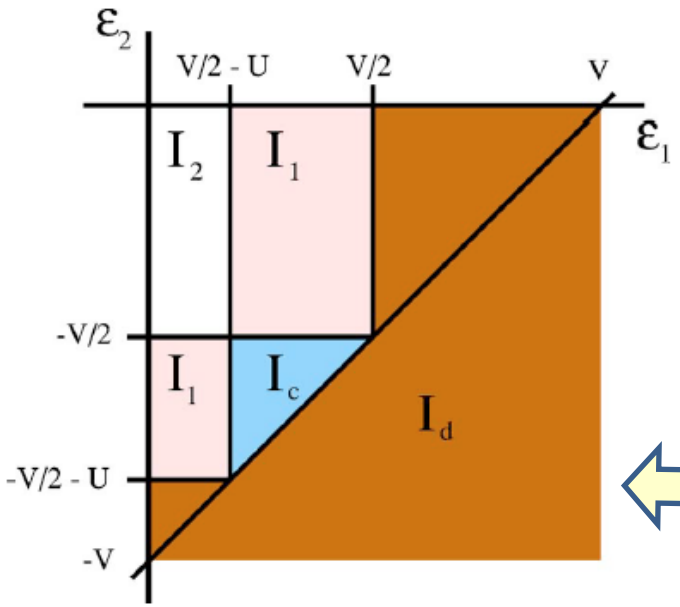

direct tunneling

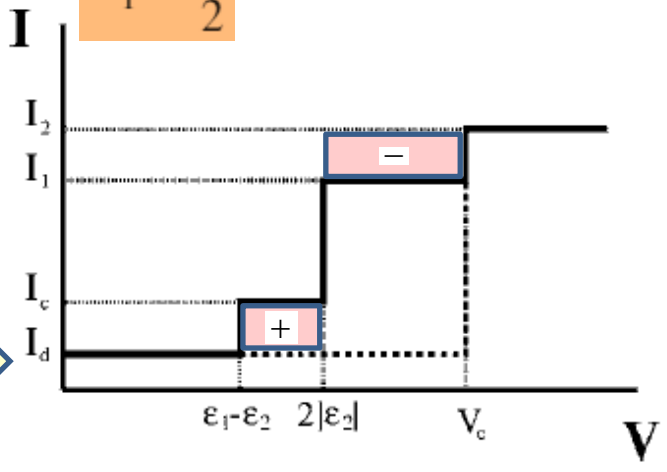

Orthodox theory of the Coulomb drag

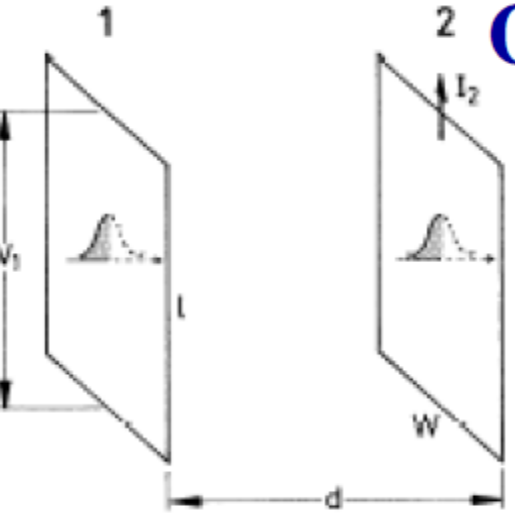

$$\dot{k}_1 \cdot \frac{\partial f_1^0}{\partial k_1} = \left[\frac{\partial f_1}{\partial t}\right]_{coll}$$

$$\hbar \dot{k}_1 = -eE_1$$

$$2\int \frac{dk_1}{(2\pi)^2} k_{1x} \frac{eE_1}{\hbar} \cdot \frac{\partial f_1^0}{\partial k_{1x}} = \sum_\sigma \int \frac{dk_1}{(2\pi)^2} k_{1x} \left[\frac{\partial f_1}{\partial t}\right]_{coll}$$

$$\frac{V_1}{I_2} = \frac{1}{W}\rho_D$$

transresistance

$$= \frac{eE_1 n_1}{\hbar} \propto V_1$$

$$\left[\frac{\partial f_1}{\partial t}\right]_{coll} \propto \int dk_2 \int dk_{1'} W(1,2;1',2') f_1^0 (1-f_{1'}^0) f_2 (1-f_{2'}) \delta(\varepsilon_1 + \varepsilon_2 - \varepsilon_{1'} - \varepsilon_{2'})$$

interlayer scattering probability

$$q = k_{1'} - k_1 = k_2 - k_{2'}$$

$$\left(f_2 - f_2^0\right) \propto k_{2x} E_2 \propto k_{2x} I_2$$

$$E_1 \propto E_2 \sum k_{1x} k_{2x} \to E_2 \sum_q q^2 \ldots.$$

A fancy way to present the final result

$$\sum_p f_p^0(1-f_{p-q}^0)\delta\left(\varepsilon_{p-q}-\varepsilon_p-\hbar\omega\right)=-\frac{\hbar\,\mathrm{Im}\,\chi(q,\omega)}{2\pi A\left(1-e^{-\beta\hbar\omega}\right)}$$

density-density response function

$$\beta=\frac{1}{T}$$

$$\rho_D=\frac{\hbar^2\beta}{\pi n_L n_R e^2 A}\sum_q q^2\int_0^\infty d\omega\left|U_e(q,\omega)\right|^2\frac{\mathrm{Im}\,\chi_L(q,\omega)\,\mathrm{Im}\,\chi_R(q,\omega)}{e^{\beta\hbar\omega}+e^{-\beta\hbar\omega}-2}$$

$$U_e(q,\omega)=\frac{V_e(q)}{\left[1+V_a(q)\chi_L(q,\omega)\right]\left[1+V_a(q)\chi_R(q,\omega)\right]-V_e^2(q)\chi_L(q,\omega)\chi_R(q,\omega)}$$

dynamically screened interaction

$$V_a(q)=\frac{2\pi e^2}{q}$$

$$V_e(q)=V_a(q)e^{-qd}$$

M.B. Pogrebinskii, Sov. Phys. Semicond. **11**, 372 (1977).

An analysis is made of the drag of carriers in one of the semiconductor films of a semiconductor–insulator–semiconductor (SIS) structure due to the direct Coulomb interaction with carriers in the other semiconductor film. The transport equations for high injection rates are used to derive a system of equations for the carrier fluxes in the films and these are solved, together with the Poisson equations, in the "film" quasineutrality approximation. Expressions are given for the carrier momentum relaxation times in the case of scattering by impurity ions and by other carriers in the system under discussion. Estimates of these relaxation times are obtained also in the model of a "two-dimensional" electron gas. A distribution is found of the carrier densities along the films. General expressions are obtained for the calculation of the current–voltage characteristics of SIS structures and it is shown that the small-current characteristics are of the Shockley type. Attention is drawn to the fact that an SIS structure behaves, in a sense, as inductance if the drag is present. Recommendations are given on the choice of the materials in which this effect may be observed.

Physica 117B & 118B (1983) 750-752
North-Holland Publishing Company

HOT ELECTRON EFFECTS IN HETEROLAYERS

Peter J. Price

IBM T.J.Watson Research Center
Yorktown Heights, NY 10598

Phenomena of interaction in the direction perpendicular to the layer planes, for hot electrons in heterolayer structures such as may be grown by molecular beam epitaxy, are discussed. In particular, energy transfer between electrons in neighboring heterolayers, due to mutual coulomb scattering, and escape of electrons from a heterolayer, due to phonon scattering processes, are analyzed; and it is shown that substantial rates are possible.

Phonons

or photons generated by an excited (hot electron) layer state may induce electron transitions in, and hence excitation of, a neighboring layer. Similarly, the charge fluctuations in the layers are a means of interaction tending to equalize drift velocities and electron temperatures in adjoining layers -- this is the "coulomb mutual scattering" (CMS) effect

There is similarly a CMS transfer of momentum, so that the current in layer 1 is proportional to $\mathscr{E}_1 + Z_{12}\sigma_2\mathscr{E}_2$ where σ and $\mathscr{E}$ are conductance "per square" and field.

Early experiment

VOLUME 66, NUMBER 9 PHYSICAL REVIEW LETTERS 4 MARCH 1991

Mutual Friction between Parallel Two-Dimensional Electron Systems

T. J. Gramila,[1] J. P. Eisenstein,[1] A. H. MacDonald,[2] L. N. Pfeiffer,[1] and K. W. West[1]
[1]*AT&T Bell Laboratories, Murray Hill, New Jersey 07974*
[2]*Department of Physics, Indiana University, Bloomington, Indiana 47405*
(Received 14 November 1990)

Frictional drag between isolated two-dimensional electron gases separated by a thin barrier has been observed at low temperatures in GaAs/AlGaAs double-quantum-well structures. Separate electrical connection to the two electron systems allows the injection of current into one and the detection of a small drag voltage across the other. The drag voltage is a direct measure of the interwell momentum relaxation rate. Measurements of this rate are in qualitative agreement with calculations of an interwell Coulomb scattering model.

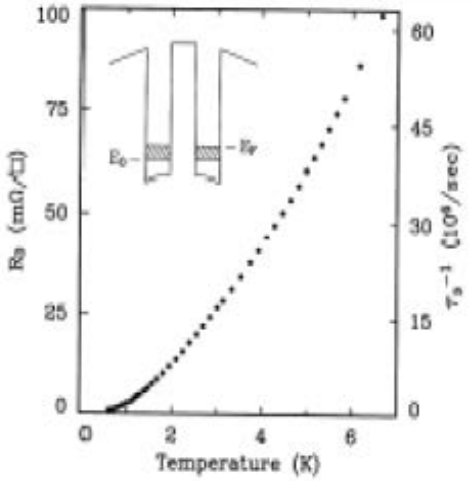

FIG. 2. Temperature dependence of observed frictional drag between two 2D electron systems separated by 175-Å barrier. Data are plotted as an equivalent resistance and a momentum-transfer rate. Inset: An idealized conduction-band diagram for a DQW structure indicating the ground subband energy E_0 and the Fermi energy E_F.

Interwell scattering rates is 1% of the mobility scattering rate

$$n = 1.5 \cdot 10^{11}\, cm^{-2}$$

$$\mu = 3.5 \cdot 10^{6}\, cm^{2}/V \cdot s$$

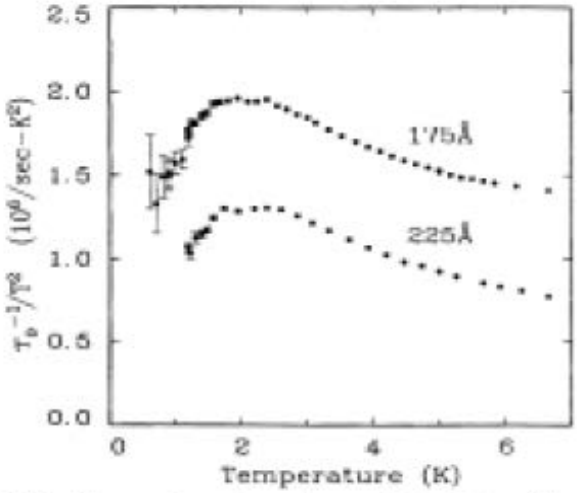

FIG. 3. Temperature dependence of the interwell momentum-transfer rate divided by T^2 for both the 175- and 225-Å barrier samples.

Coupled Electron-Hole Transport

U. Sivan,[a] P. M. Solomon, and H. Shtrikman[b]

IBM Research, T. J. Watson Research Center, P.O. Box 218, Yorktown Heights, New York 10598

(Received 7 August 1991)

We report on transport measurements in a novel system composed of two parallel 2D electron and hole gases separated by a barrier which is high enough to prevent tunneling and recombination while thin enough to allow for strong interlayer Coulomb interaction. Separate electrical contacts to each layer and independent control of both carrier densities facilitate a detailed study of the electron-hole interaction. Current driven in one layer is found to induce opposite current in the other layer. The measured electron-hole momentum-transfer rate is a factor of 5 to an order of magnitude larger than in previous experiments on electron-electron scattering and calculations based on Coulomb scattering theory.

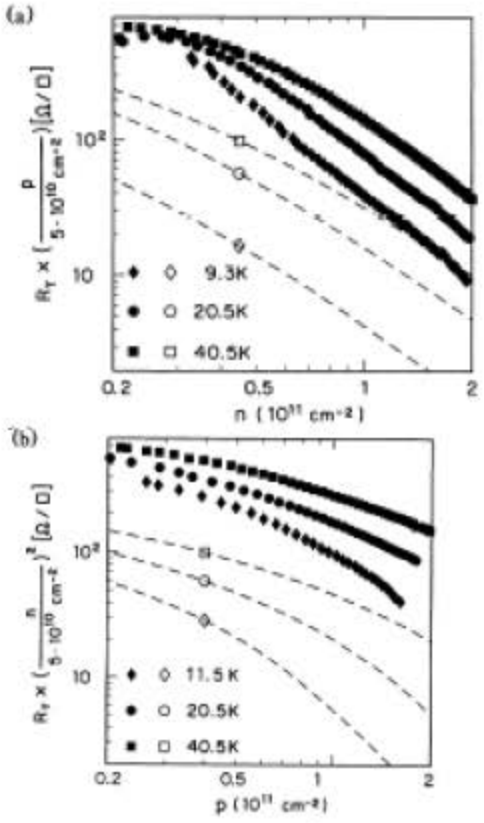

FIG. 2. (a) Corrected transimpedance per square vs electron concentration for three temperatures, $p=5\times10^{10}$ cm^{-2}. Solid and open symbols correspond to experimental and theoretical results, respectively. (b) Corrected transimpedance per square vs hole concentration, $n=5\times10^{10}$ cm^{-2}.

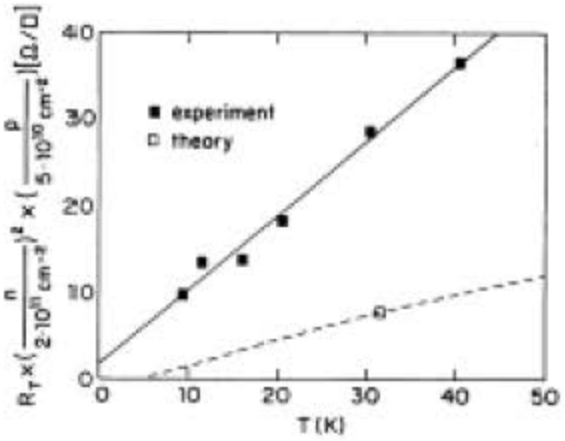

FIG. 3. $R_T[n/(2\times10^{11}\ \text{cm}^{-2})]^2 p/(5\times10^{10}\ \text{cm}^{-2})$ vs temperature for $p=5\times10^{10}$ cm^{-2} and $n=2\times10^{11}$ cm^{-2}. Solid and open symbols correspond to experimental and theoretical results, respectively (dashed line is for $p=5\times10^{10}$ cm^{-2} and $n=2\times10^{11}$ cm^{-2}). The solid line is a best fit to the experimental data.

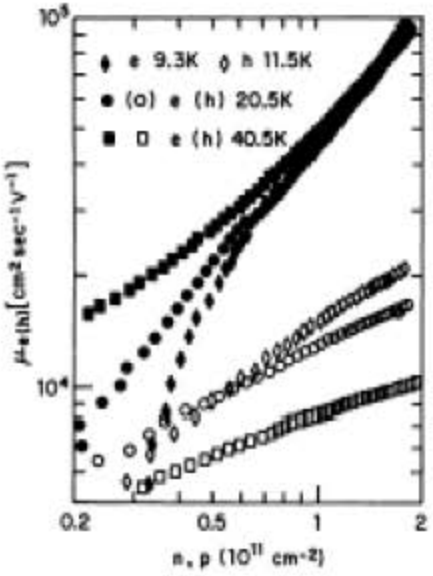

FIG. 4. Electron and hole mobilities vs carrier concent for three temperatures and the same conditions as in Fig.

Transition into an insulating phase occurs at T<9K and

$$n \leq 5 \bullet 10^{10}\, cm^{-2}$$

Layers with localized electrons

VOLUME 89, NUMBER 10 PHYSICAL REVIEW LETTERS 2 SEPTEMBER 2002

Coulomb Drag for Strongly Localized Electrons: A Pumping Mechanism

1. Momentum is not a good quantum number

2. Description in terms of spatially averaged response functions is inadequate because of exponentially wide spread in the local transition frequencies

Instead of momentum exchange due to collisions, the coupling between strongly localized systems is due to energy shifts in the passive layer caused by electron hops in the active layer and vice versa

This shifts "communicate" the overall direction of current from the active to the passive layer due to correlated character of electron hops

A minimal model

active layer

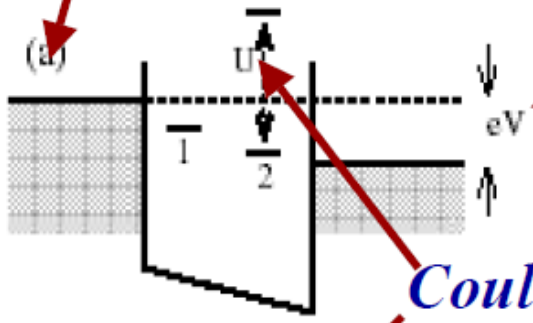

applied bias

Coulomb shift caused by occupation of the first site

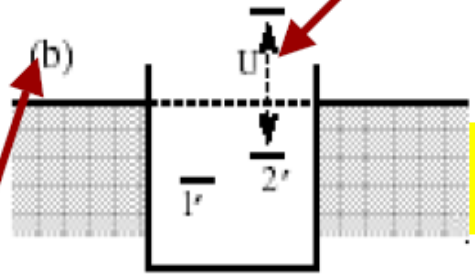

passive layer

$$K(\tau) = \langle n_1(t) n_2(t+\tau) \rangle$$

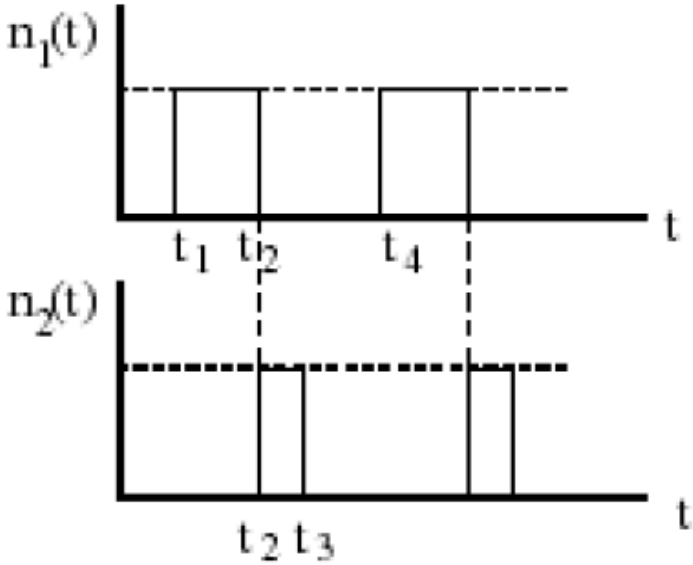

Schematic time evolution of the population of the sites 1 and 2, respectively, under conditions of a finite current

$K(\tau) = K(-\tau)$ *in equilibrium*

hops occur preferentially from 1 to 2, hence

Asymmetry analogous to the current-induced asymmetry between q and –q in the thermal density fluctuations in the metallic regime →

$$K(\tau) > K(-\tau)$$

Nonlinear regime: eV>>T ⟶ *transport is by activationless hops*

For $\varepsilon_{1,2} + U > E_F + eV$

only a single sequence of hops is possible in the active layer:

n_1 $1 \to 0 \to 0 \to 1$

n_2 $0 \to 1 \to 0 \to 0$

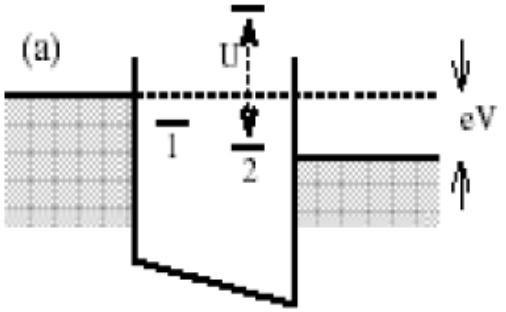

Average current through the active layer:

$$\langle I_a \rangle = \frac{e}{\tau_1 + \tau_2 + \tau_3}$$

waiting times for transitions $l \to 1, 1 \to 2, 2 \to r$ *respectively*

Response of the passive layer to a single cycle in the active layer

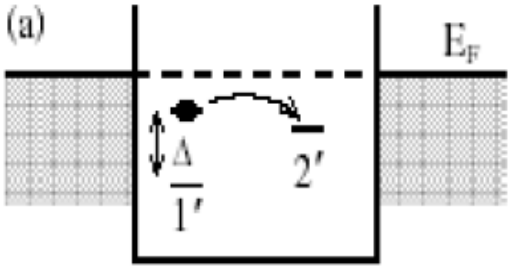

1. *When the site 1 is occupied, the only hop that can occur in the passive layer is:* $1' \to 2'$ *provided that the site* $1'$ *is shifted above* $2'$*, but remains below* E_F

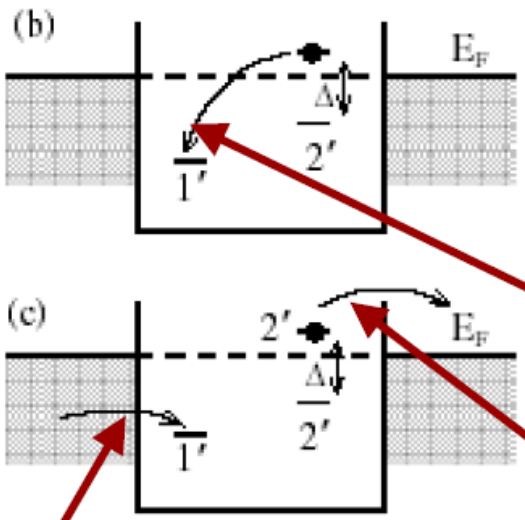

2. *If the hop* $1' \to 2'$ *took place while the site 1 was occupied, then two transitions within the passive layer become possible after the hop* $1 \to 2$

(i) *The electron from the site* $2'$ *goes back to* $1'$

(ii) *The electron from the site* $2'$ *tunnels into the right contact. As a result, the site* $1'$ *gets unblocked allowing an electron from the right contact to tunnel on* $1'$

In the case (i), *the passive layer returns to the initial state after the cycle in the active layer*

In the case (ii), *if both tunneling events occurred, the cycle in the active layer results in the transfer of an electron in the passive layer from left to right.* *This is nothing but the drag current!*

Calculation of the drag current

Simplest case: hops $1 \to 2$ *and* $1' \to 2'$ *constitute the "bottlenecks", i.e.,*

$\tau_1, \tau_3 \ll \tau_2$ $\quad$ $T_1, T_3 \ll T_2$

Average waiting times for transitions

$l \to 1', 1' \to 2', 2' \to r$

Probability that $1' \to 2'$ *occurs during a cycle in the active layer*

$$p = \int_0^\infty dt \left[1 - \exp\left(-\frac{t}{T_2} \right) \right] P_{1\to 2}(t) = \frac{\tau_2}{\tau_2 + T_2}$$

$$P_{1\to 2}(t) = \frac{1}{\tau_2} \exp\left(-\frac{t}{\tau_2} \right)$$

Distribution of the waiting times for the transition $1 \to 2$

$$\langle I_d \rangle = p \langle I_a \rangle \approx \frac{e}{\tau_2 + T_2}$$

As a result of the correlated character of transport, the drag current is comparable to the current in the active layer, $\langle I_a \rangle \approx \frac{e}{\tau_2}$

Analogy: Classical electron pump

Physica B 169 (1991) 573-574
North-Holland

SINGLE ELECTRON PUMP FABRICATED WITH ULTRASMALL NORMAL TUNNEL JUNCTIONS

H. POTHIER, P. LAFARGE, P.F. ORFILA, C. URBINA, D. ESTEVE and M. H. DEVORET

DSM/SPSRM, CEN Saclay, 91191 Gif-sur-Yvette Cedex, France

We have designed and operated a device through which single electrons can be "pumped" reversibly. It consists of a linear array of three tunnel junctions voltage biased below the Coulomb gap. Phase shifted ac voltages applied to two gates pump one electron per cycle.

tunnel junctions

quantized current

occupation of the islands

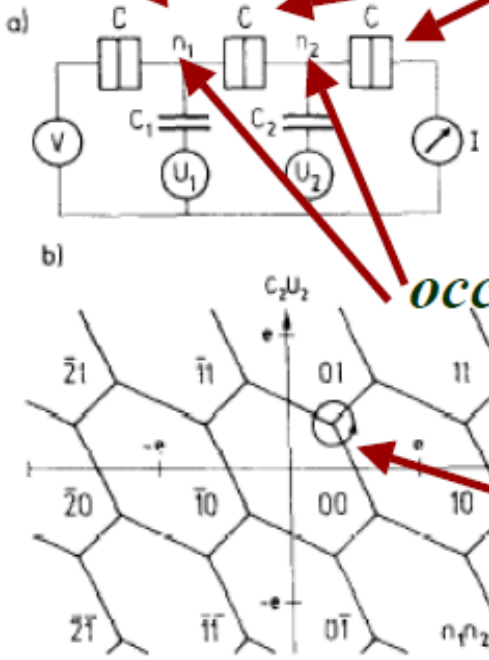

a) Circuit diagram of the electron pump. The double boxes represent the ultrasmall tunnel junctions.
b) Ground state configuration diagram at V = 0.

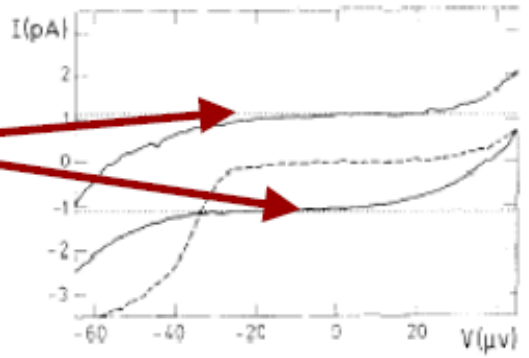

FIGURE 3
Current-voltage characteristics without ac signals on the gates (dashed line) and with ac gate voltages at f = 7 MHz corresponding to two opposite rotation senses around point P of Fig. 2 (full lines). Dotted lines correspond to expected current values I = +e × f.

the system evolves sequentially through (0,0), (1,0), (0,1) *and back to* (0,0)

At each transition one particular junction lets one electron through

Pumping due to phase-shifted rf modulation of the barrier heights

VOLUME 67, NUMBER 12 PHYSICAL REVIEW LETTERS 16 SEPTEMBER 1991

Quantized Current in a Quantum-Dot Turnstile Using Oscillating Tunnel Barriers

L. P. Kouwenhoven, A. T. Johnson, N. C. van der Vaart, and C. J. P. M. Harmans
Faculty of Applied Physics, Delft University of Technology, P.O. Box 5046, 2600GA Delft, The Netherlands

C. T. Foxon
Philips Research Laboratories, Redhill, Surrey RH15HA, United Kingdom
(Received 20 May 1991)

We have observed a quantized current in a lateral quantum dot, defined by metal gates in the two-dimensional electron gas (2DEG) of a GaAs/AlGaAs heterostructure. By modulating the tunnel barriers in the 2DEG with two phase-shifted rf signals, and employing the Coulomb blockade of electron tunneling, we produced quantized current plateaus in the current-voltage characteristics at integer multiples of ef, where f is the rf frequency. This demonstrates that an integer number of electrons pass through the quantum dot each rf cycle.

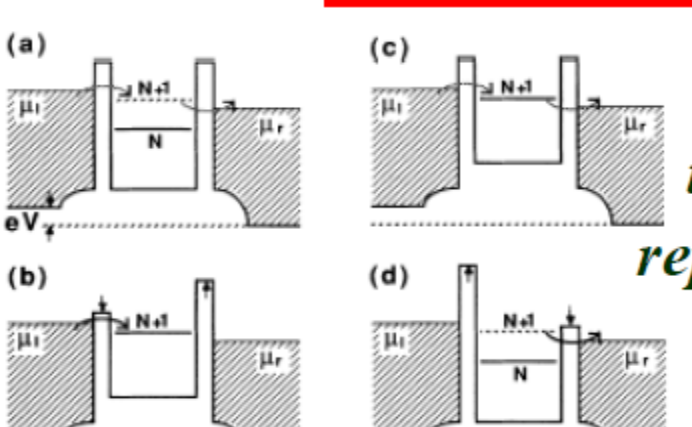

FIG. 1. Potential landscape through the quantum dot. μ_l and μ_r are the electrochemical potentials of the left and right reservoirs, and $V=(\mu_l-\mu_r)/e$ is the bias voltage. The level N indicates $\mu_d(N)$ and N electrons are confined in the quantum dot, while the level $N+1$ indicates $\mu_d(N+1)$. (a)–(d) are four stages of a rf cycle where the probability for electron tunneling is large when the barrier is low (solid arrows), and small when

in hopping drag, the pulses $n_1(t), n_2(t)$ replace the rf signals; the phase shift is determined by the direction of current in the active layer

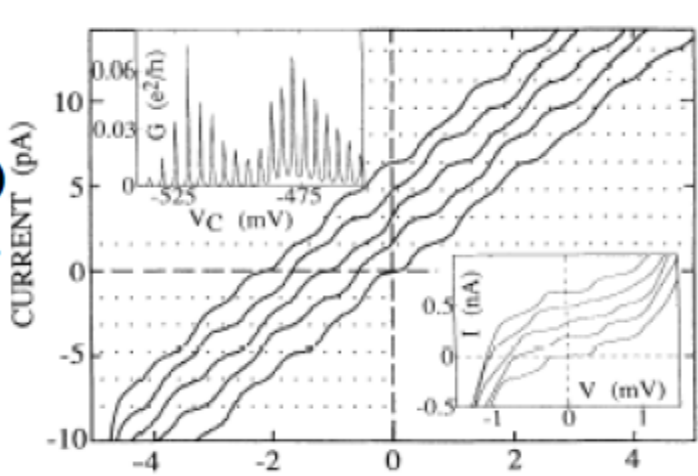

FIG. 2. Main figure: I-V characteristics when two phase-shifted rf signals are applied with a frequency $f=10$ MHz, showing current plateaus at integer multiples of ef (dotted lines). The curves correspond to different center-gate voltges and are offset for clarity by an integer times ef. Upper inset: Coulomb conductance oscillations vs center-gate voltage. Lower inset: Coulomb staircase in the I-V characteristics (the curves correspond to different center-gate voltages and are

Effect of a weak magnetic field on the electrical conductivity of polyacetylene films

E. L. Frankevich, I. A. Sokolik, D. I. Kadyrov, and V. M. Kobryanskiĭ
Institute of Chemical Physics, Academy of Sciences of the USSR

Pis'ma Zh. Eksp. Teor. Fiz. **36**, No. 11, 401–403 (5 December 1982)

A decrease in the electrical conductivity of polyacetylene films when an external magnetic field is switched on, saturating in fields $H \gtrsim 100$ Oe, is observed. The effect is explained by the dependence of the hopping probability of current carriers along soliton levels on the spin state of polaron-soliton paramagnetic particle pairs.

"The study of the effect of magnetic field on chemical reactions has long been a romping ground for charlatans"
P.W. Atkins, Chem. in Britain, 12, 214 (1976).

Pioneering papers on OMAR

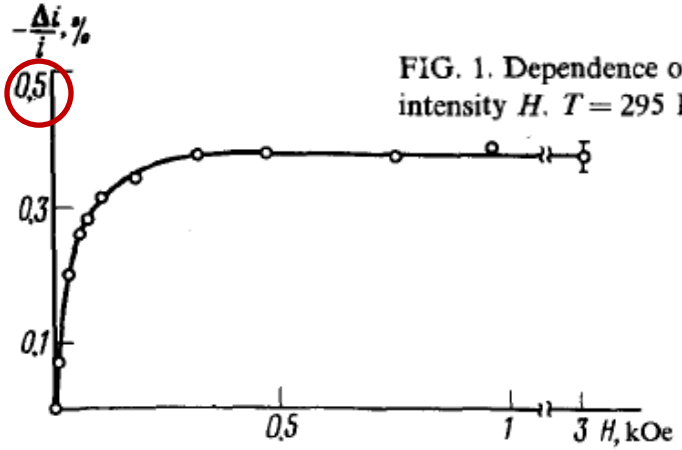

FIG. 1. Dependence of the relative change in current $\Delta i/i$ through a $(CH)_x$ specimen on the magnetic field intensity H. $T = 295$ K.

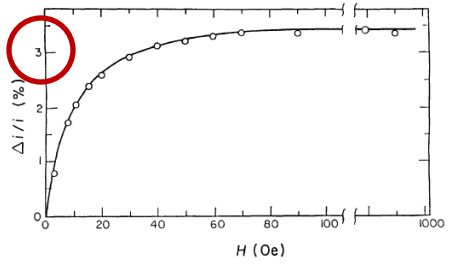

FIG. 2. Typical dependence of the photocurrent i on the magnetic-field strength H for films of PPV, DMOP-PPV, and PPPV. The data deputed here are for PPPV film.

PHYSICAL REVIEW B VOLUME 46, NUMBER 15 15 OCTOBER 1992-I

Polaron-pair generation in poly(phenylene vinylenes)

E. L. Frankevich and A. A. Lymarev I. Sokolik and F. E. Karasz S. Blumstengel
R. H. Baughman H. H. Hörhold

The hyperfine interaction (HFI) in one or in both pair members mixes the singlet and triplet states, the degree of mixing being dependent on the external magnetic field.

$$\hat{H} = 2g\hat{S}H + \hbar a_1 I\hat{S}_1 + \hbar a_2 I\hat{S}_2 - \hbar J(r)(\tfrac{1}{2} - 2\hat{S}_1\hat{S}_2)$$

PHYSICAL REVIEW B 72, 205202 (2005)

Large magnetoresistance in nonmagnetic π-conjugated semiconductor thin film devices

Ö. Mermer,[1] G. Veeraraghavan,[2] T. L. Francis,[2,3] Y. Sheng,[1] D. T. Nguyen,[1] M. Wohlgenannt,[1,*] A. Köhler,[4] M. K. Al-Suti,[5] and M. S. Khan[5]

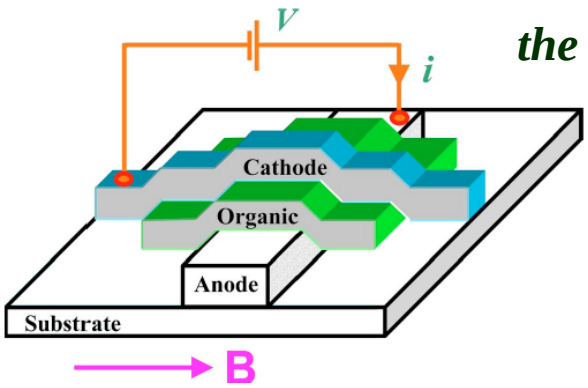

the device area $\approx 10\,\mathrm{mm}^2$

FIG. 2. Magnetoresistance, $\Delta R/R$ curves, measured at room temperature in an ITO/PEDOT/polyfluorene(≈100 nm)/Ca device at different voltages. The inset shows the device resistance as a function of the applied voltage.

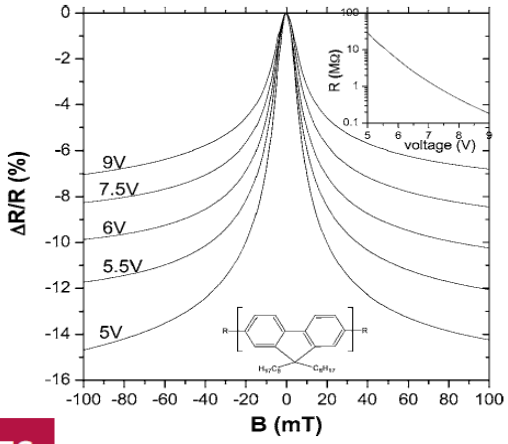

OMAR is due to hyperfine fields

nature materials
ARTICLES
PUBLISHED ONLINE: 14 FEBRUARY 2010 | DOI: 10.1038/NMAT2633

Isotope effect in spin response of π-conjugated polymer films and devices

Tho D. Nguyen[1], Golda Hukic-Markosian[1], Fujian Wang[1], Leonard Wojcik[1], Xiao-Guang Li[2], Eitan Ehrenfreund[3] and Z. Valy Vardeny[1]*

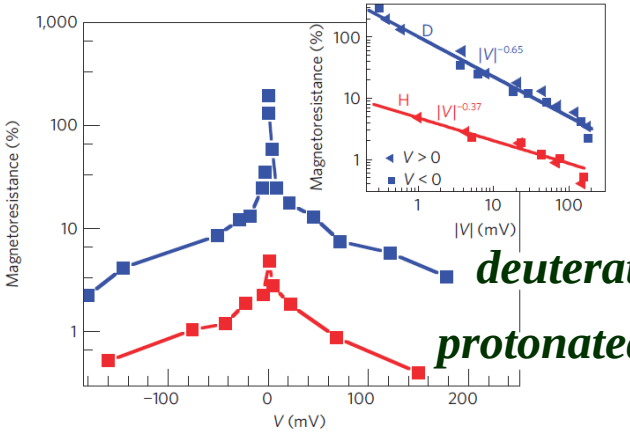

deuterated

protonated

organic spin-valve

LSMO (200 nm)/DOO-PPV(25 nm)/Co(15 nm)

ferromagnetic electrodes

Weak localization and antilocalization in semiconducting polymer sandwich devices

Ö. Mermer and M. Wohlgenannt*
Department of Physics and Astronomy, The University of Iowa, Iowa City, IA 52242-1479
G. Veeraraghavan, T. L. Francis
Department of Electrical and Computer Engineering, The University of Iowa, Iowa City, IA 52242-1595
(Dated: February 2, 2008)

arXiv: cond-mat /0312204

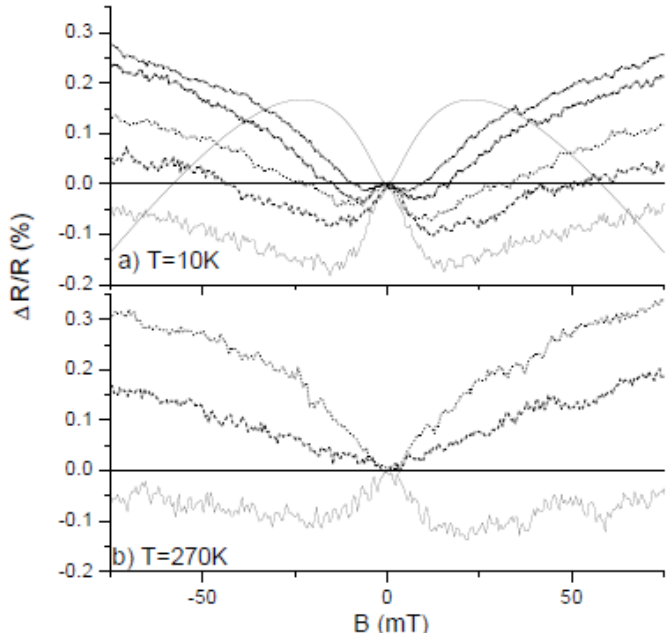

FIG. 2: Examples of MR, $\Delta R/R$ traces close to the transition between WL and WAL in a Au/PFO ($\approx$ 150 nm)/Al device measured at 10 K (panel a)) and 270 K (panel b)). The solid line is calculated using (equ. 2).

the observed MR traces closely resemble MR traces due to weak localization (WL, negative MR) and weak antilocalization (WAL, positive MR) well known from the study of diffusive transport in metals and semiconductors [10, 11, 12]. This suggests analyzing the MR data using the theory of weak localization. In the following we present strong evidence in support of this interpretation. We note that in principle there are several mechanisms yielding positive MR, such as Lorentz force, hopping magnetoresistance [16] and electron-electron interaction [17], but we are unaware of another mechanism, other than WL, that gives weak-field negative MR.

VOLUME 90, NUMBER 7 PHYSICAL REVIEW LETTERS week ending 21 FEBRUARY 2003

Gate-Controlled Spin-Orbit Quantum Interference Effects in Lateral Transport

J. B. Miller,[1,2] D. M. Zumbühl,[1] C. M. Marcus,[1] Y. B. Lyanda-Geller,[3] D. Goldhaber-Gordon,[1,4] K. Campman,[5] and A. C. Gossard[5]

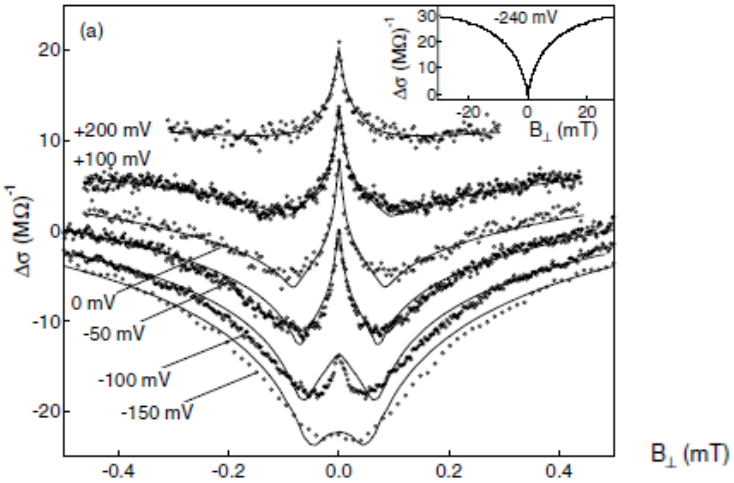

Feature at very small fields

PRL 105, 166804 (2010) PHYSICAL REVIEW LETTERS week ending 15 OCTOBER 2010

Magnetoconductance Response in Unipolar and Bipolar Organic Diodes at Ultrasmall Fields

T. D. Nguyen,[1] B. R. Gautam,[1] E. Ehrenfreund,[1,2] and Z. V. Vardeny[1,*]

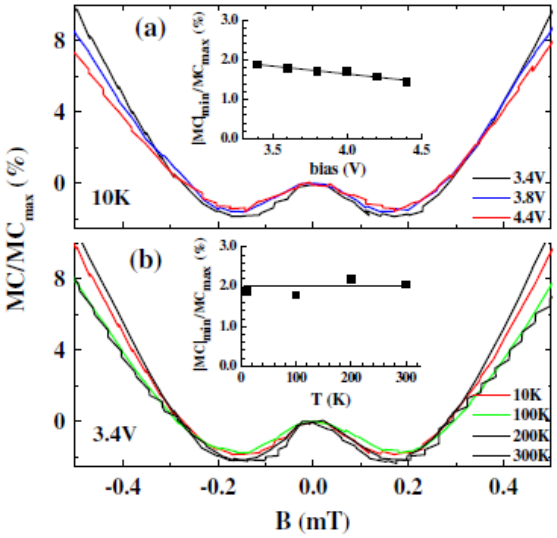

$$H_{Zeeman} = \mu_B(g_1\vec{S}_1 + g_2\vec{S}_2)\cdot\vec{B}$$

$$H_{HF} = \sum_{i=1}^{2}\sum_{j=1}^{N_i}\vec{S}\cdot(a_{ij} + \tilde{A}_{ij})\cdot\vec{I}_{ij}$$

$$H_R = -\frac{i\hbar}{2}\gamma_S P^S - \frac{i\hbar}{2}\gamma_T P^T$$

where $P^{S,T}$ is the singlet (triplet) projection operator.

$$\sigma(t) = \exp(-iHt/\hbar)\sigma(0)\exp(iH^{\dagger}t/\hbar)$$

$$\rho_\alpha(t) = Tr(P^\alpha\sigma(t)) = \frac{4}{M}\sum_{n,m}P^\alpha_{n,m}\sigma_{m,n}(0)\exp[i(E^*_m - E_n)t/\hbar]$$

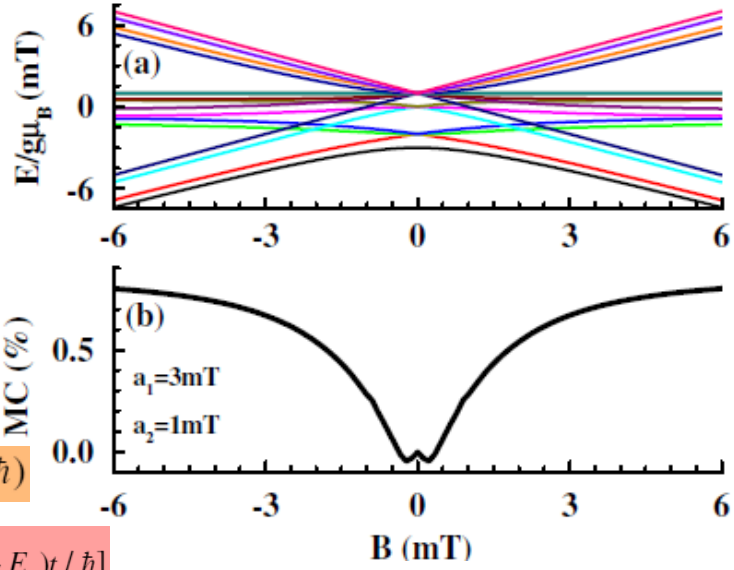

both carriers are coupled to one proton

FIG. 3 (color online). Normalized MC(B) response of a bipolar diode based on D-DOO-PPV for $|B| < 0.5$ mT at (a) various bias voltages at $T = 10$ K, and (b) various temperatures at $V = 3.4$ V; MC_{max} is defined in Fig. 1. The insets in (a) and (b), respectively, summarize MC_{min}/MC_{max} at various voltages at 10 K, and various temperatures at 3.4 V.

$$E_n = \hbar(\omega_n - i\gamma_n)$$

$$\gamma_{nm} = \gamma_n + \gamma_m$$

FIG. 4 (color online). (a) Example of calculated energy levels vs B for a spin pair with isotropic HFI; $a_1/g\mu_B = 3a_2/g\mu_B = 3$ mT, $J = 0$. Note the multiple level crossing at $B = 0$. (b) Calculated MC(B) response for a SP with axially symmetric HFI averaged over all magnetic field directions. The isotropic HFI is the same as in (a). The anisotropic HFI is $a_{zz} = 0.15a_i$ for the respective SP constituent.

the time dependent dissociated fraction of either the singlet or triplet is $k_{\alpha D}\rho_\alpha(t)$

$$\Phi_{\alpha D} = \int_0^\infty k_{\alpha D}\rho_\alpha(t)dt = \frac{4}{M}\sum_{n,m}P^\alpha_{n,m}\sigma_{m,n}(0)\frac{k_{\alpha D}\gamma_{nm}}{\gamma^2_{nm} + \omega^2_{nm}}$$

$$MC(B) = \frac{\Phi_D(B) - \Phi_D(0)}{\Phi_D(0)}$$

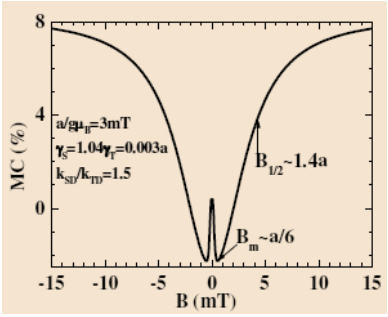

feature at $g\mu_B B \sim \gamma << a$

Dynamic Spin Chemistry

$$H_i = \vec{\omega}_0 \cdot \vec{S}_i + \sum_k a_{ik} \vec{I}_{ik} \cdot \vec{S}_i$$

Klaus Schulten and Peter G. Wolynes

Semiclassical description of electron spin motion in radicals including the effect of electron hopping

J. Chem. Phys. 68(7), 1 Apr. 1978

With large number of nuclei surrounding a radical the hyperfine field is classical with gaussian distribution

$$\vec{\omega}_i = \vec{\omega}_0 + \vec{I}_i$$

$$\vec{I}_i = \sum_k a_{ik} \vec{I}_{ik}$$ ⇐ *local hyperfine field*

$$f(I_i) = \left(\frac{\tau_i^2}{4\pi}\right)^{3/2} \exp\left(-\frac{I_i^2 \tau_i^2}{4\pi}\right)$$

$$\frac{1}{\tau_i} = \frac{1}{6} \sum_k a_{ik}^2 I_{ik} (I_{ik} + 1)$$

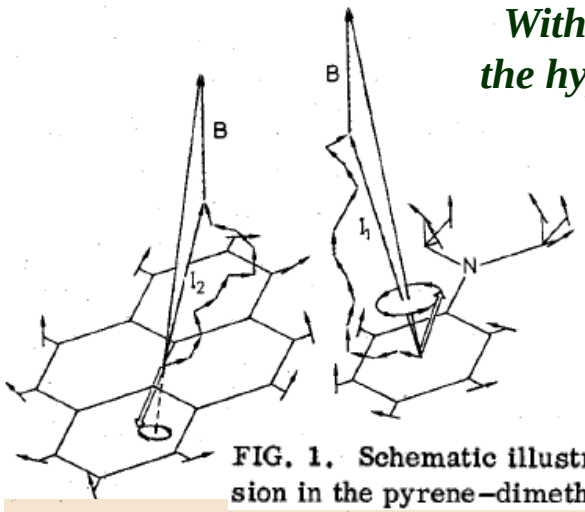

FIG. 1. Schematic illustration of the electron spin precession in the pyrene–dimethylaniline ($^2Py^- + {}^2DMA^+$) radical pair.

a pair is initially in a singlet state

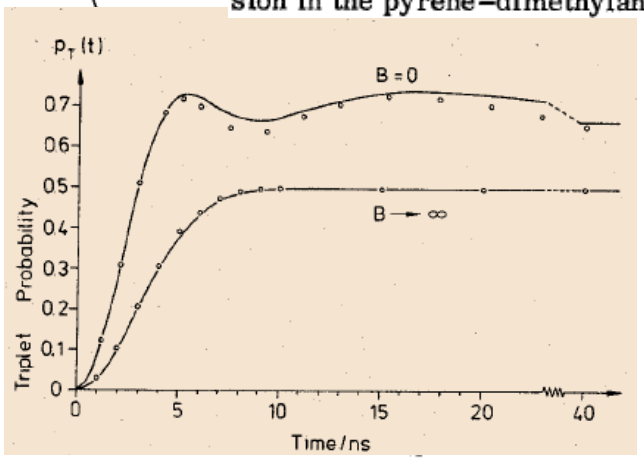

FIG. 2. Comparison of the triplet probability of the unpaired electron spins in $^2Py^- + {}^2DMA^+$ predicted by the semiclassical approximation, i.e., Eqs. (31) and (33), [—] and evaluated from an exact quantum mechanical analysis (Ref. 4) [o]. Hyperfine coupling constants assumed are Py: $4\times(a_H = 2.3$ G), $4\times(a_H = 5.2$ G); DMA: $6\times(a_{CH_3} = 12.0$ G), $1\times(a_N = 12.0$ G), $3\times(a_H = 6.25$ G).

Averaged (over hyperfine fields) probability to find a pair in the triplet state

$$p_{ST}(t) = \frac{1}{2}\left[1 - \exp\left(-b_e^2 t^2 - b_h^2 t^2\right)\right], \; B >> b_e, b_h$$

$$p_{ST}(t) = \frac{3}{4}\left[1 - F(b_e t) F(b_h t)\right], \; B << b_e, b_h$$

$$F(z) = \frac{1}{3}\left[1 + 2\left(1 - 2z^2\right)\exp\left(-z^2\right)\right]$$

Bipolaron Mechanism for Organic Magnetoresistance

P. A. Bobbert,[1,2] T. D. Nguyen,[3] F. W. A. van Oost,[1,2] B. Koopmans,[2] and M. Wohlgenannt[3,*]

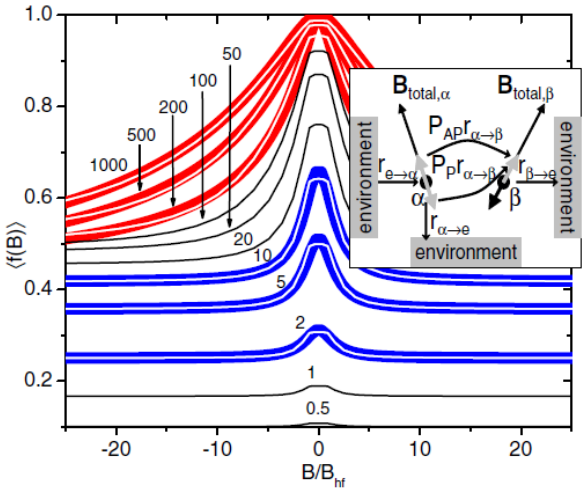

FIG. 1 (color online). Hyperfine field average of the function $f(B)$ of Eq. (2), determining the bipolaron probability, for various branching ratios $b = r_{\alpha\to\beta}/r_{\alpha\to e}$. The lower three thick lines show Lorentzian fits, the upper three fits to the non-Lorentzian empirical law. Inset: model as described in the main text, with the black arrow indicating the spin of a polaron present at β (arbitrarily chosen opposite to the local magnetic field) and the gray arrows the spin of a possible additional polaron.

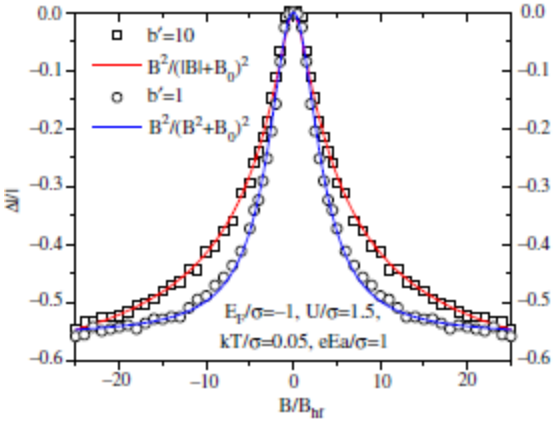

FIG. 2 (color online). Symbols: ○, simulated magnetoconductance traces for a particular choice of parameters. □, bipolaron formation and dissociation rates multiplied by $b' = 10$. Solid lines: fits through □ and ○ with the empirical laws $\propto B^2/(|B| + B_0)^2$ ($B_0 \approx 2.75B_{\rm hf}$) and $\propto B^2/(B^2 + B_0^2)$ ($B_0 \approx 3.5B_{\rm hf}$), respectively.

Because of strong on-site exchange effects [9,10], we can assume that bipolarons occur only as spin singlets. Two polarons having the same spin component along a common quantization axis have zero singlet probability and cannot form a bipolaron. This "spin blocking" is the basic notion of our mechanism.

$$p_\beta = \frac{r_{e\to\alpha}}{r_{\beta\to e}} f(B) p \qquad f(B) \equiv \frac{P_{\rm P}P_{\rm AP} + 1/(4b)}{P_{\rm P}P_{\rm AP} + 1/(2b) + 1/b^2}$$

The singlet probability is now given by [13]

$$P = 1/4 - \mathbf{S}_i \cdot \mathbf{S}_j/\hbar^2, \qquad (1)$$

where $\mathbf{S}_{i,j}$ are the classical spin vectors pointing along $\mathbf{B}_{{\rm total},i,j}$, and $\hbar$ is Planck's constant. A straightforward analysis of this formula shows that for $B = 0$ the pairs have an average singlet probability $P = 1/4$, whereas for large field this probability is either $P_{\rm P} = 0$ or $P_{\rm AP} = 1/2$ for parallel and antiparallel pairs, respectively. We note that the notion of parallel and antiparallel pairs has its usual meaning only for large B, whereas for small B we denote as "parallel" a pair whose spins both point "up" or both "down" along the local field axes, which are randomly oriented.

A basic physical picture of OMAR

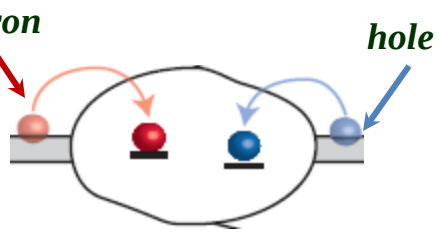

I. Bipolar device: current is passed via e-h recombination

II. Electron and hole recombine only when their spins are in the singlet state

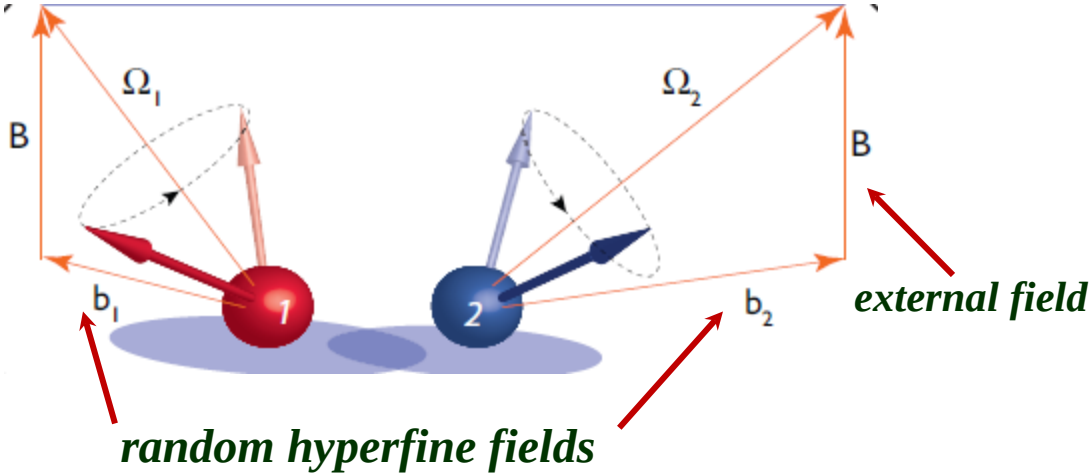

Hamiltonian of a spin pair:

$$\hat{H} = \vec{\Omega}_1 \cdot S_1 + \vec{\Omega}_2 \cdot S_2$$

$$\vec{\Omega}_1 = \vec{b}_1 + \vec{B} \qquad \vec{\Omega}_2 = \vec{b}_2 + \vec{B}$$

Dynamics of a pair contains harmonics

with frequencies $\Sigma = |\vec{\Omega}_1| + |\vec{\Omega}_2|$ *and* $\Delta = |\vec{\Omega}_1| - |\vec{\Omega}_2|$

A crucial question for OMAR: why recombination time averaged over random hyperfine fields remains sensitive to B *?*

Answer: Two specific sparse configurations of hyperfine fields give rise to anomalously long recombination times

I. Effective fields $\vec{\Omega}_1$ *and* $\vec{\Omega}_2$ *are either parallel or antiparallel*

Then a pair created in the state different from singlet will never recombine

II. $|\vec{\Omega}_1| = |\vec{\Omega}_2|$ *(soft pair) will never cross from* T_0 *to* S

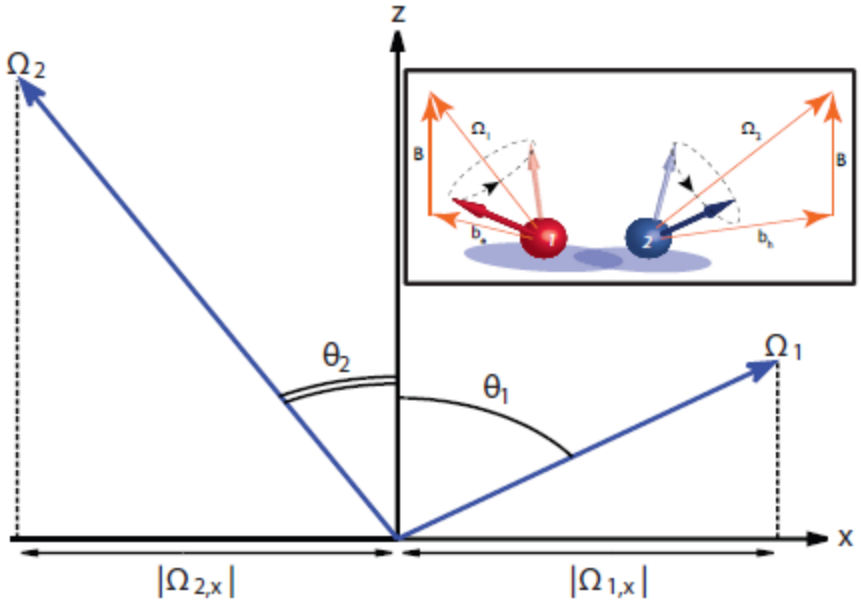

Natural choice of the quantization axis for $|\vec{\Omega}_1| = |\vec{\Omega}_2|$ *is along the bisector*

"Trapping" configurations block the current

Essence of OMAR: change of the number of "trapping" configurations with B

Simplest transport model of parallel channels:

quantitative relation between recombination and current

Assembly of a pair followed by recombination constitutes a cycle ⇨ $I_n = \dfrac{1}{\langle t_n \rangle}$

cycle duration averaged over the initial states of the pair

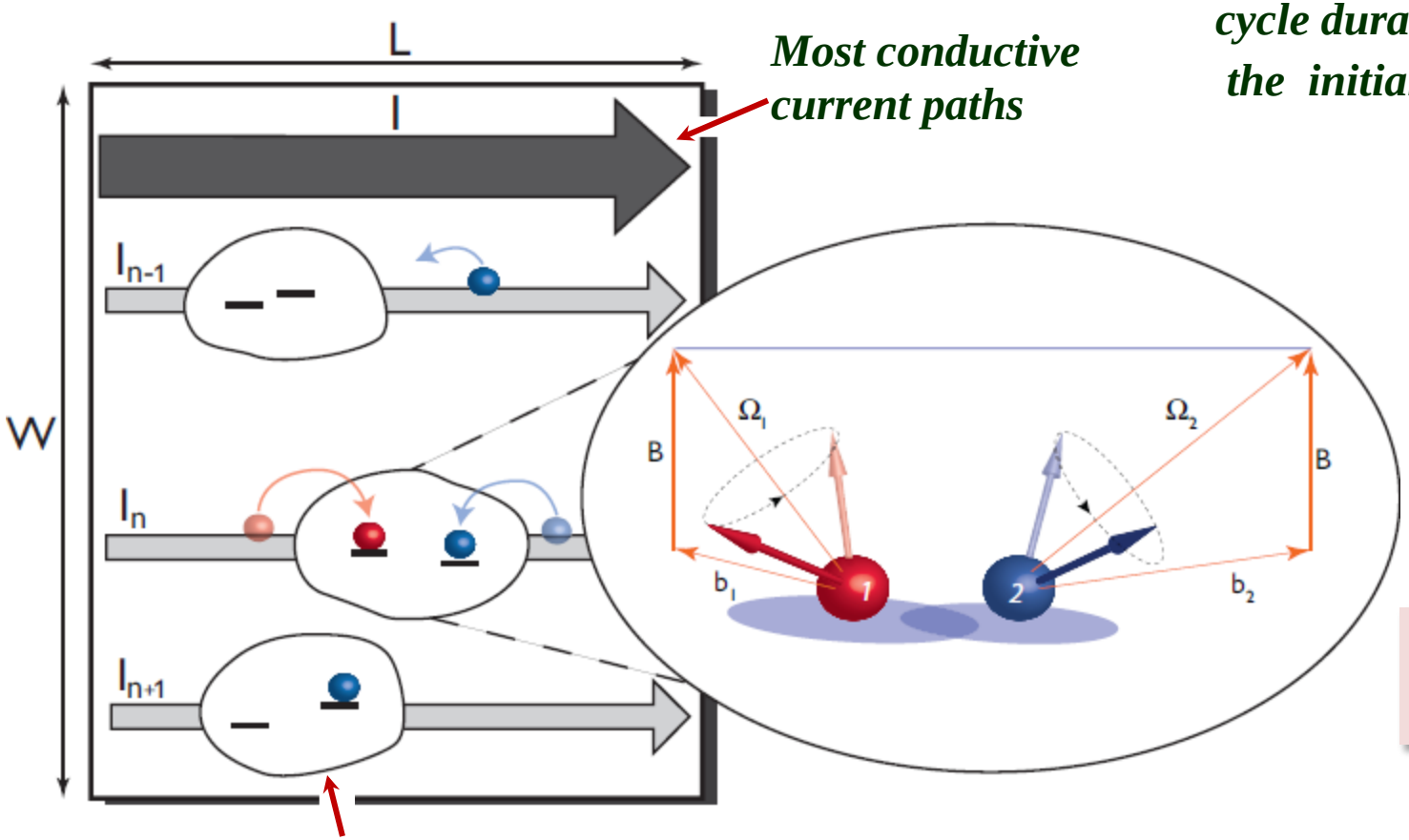

Most conductive current paths

Most resistive junction within a given path

How does the concentration of soft pairs evolve with B?

$$P_S(B) = \frac{1}{\pi^3 \tau b_0^6} \int d^3 b_1 \int d^3 b_2 \, \delta\left(|\vec{\Omega}_1| - |\vec{\Omega}_2|\right) \exp\left(-\frac{|\vec{b}_1|^2 + |\vec{b}_2|^2}{b_0^2}\right)$$

Counting Soft Pairs

Density of soft pairs

can be fitted well with $2 + \frac{1}{1 + 1.75x^2}$

poorer fit with $\exp\left(-0.8x^2\right)$

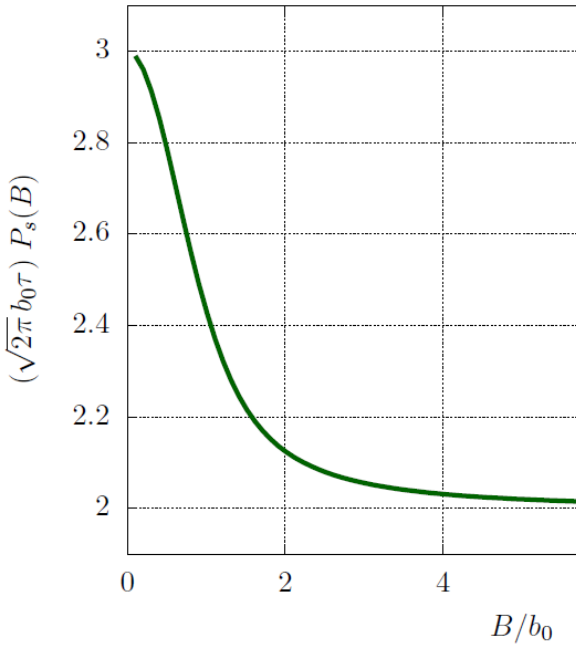

Performing the 6-fold integration,

$$P_S(B) = \frac{1}{2\sqrt{2\pi}(b_0\tau)} \left\{ 4 + \frac{b_0^2}{B^2} \left[1 - \exp\left(-\frac{2B^2}{b_0^2}\right) \right] \right\}$$

it is more likely to find a soft pair in a weak field

$$P_S(0) = \frac{3}{\sqrt{2\pi}(b_0\tau)}$$

$$P_S(\infty) = \frac{2}{\sqrt{2\pi}(b_0\tau)}$$

Dynamics of a non-interacting pair

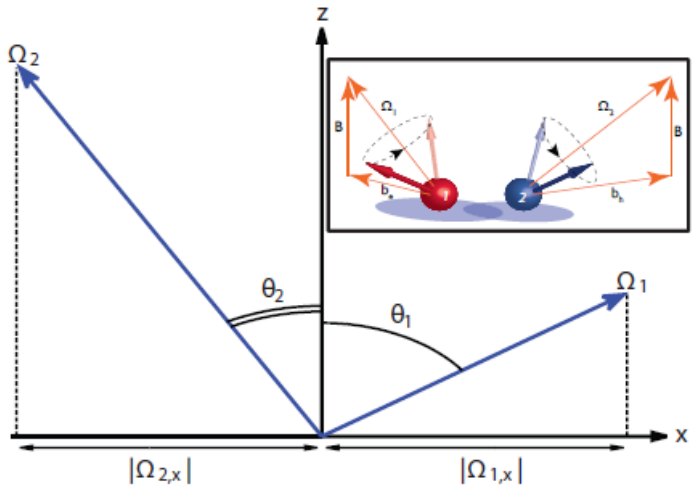

Preferential coordinate system

$\vec{\Omega}_1, \vec{\Omega}_2$ *reside in the* $xz-$ *plane*

Direction of the quantization axis is determined by the condition $\vec{\Omega}_{1x} = -\vec{\Omega}_{2x}$

$$\tan\theta_1 = \frac{|\vec{\Omega}_1 \times \vec{\Omega}_2|}{\vec{\Omega}_2^2 + \vec{\Omega}_1 \cdot \vec{\Omega}_2} \qquad \tan\theta_2 = \frac{|\vec{\Omega}_1 \times \vec{\Omega}_2|}{\vec{\Omega}_1^2 + \vec{\Omega}_1 \cdot \vec{\Omega}_2}$$

Equations of motion for a pair:

$$i\frac{\partial S}{\partial t} = \Delta_z T_0 - \frac{1}{\sqrt{2}}\Delta_x T_+ + \frac{1}{\sqrt{2}}\Delta_x T_-$$

$$\Delta_z = \frac{\vec{\Omega}_{1z} - \vec{\Omega}_{2z}}{2} \qquad \Delta_x = \frac{\vec{\Omega}_{1x} - \vec{\Omega}_{2x}}{2}$$

$$i\frac{\partial T_-}{\partial t} = -\Sigma_z T_- + \frac{1}{\sqrt{2}}\Delta_x S \qquad i\frac{\partial T_0}{\partial t} = \Delta_z S \qquad i\frac{\partial T_+}{\partial t} = \Sigma_z T_+ - \frac{1}{\sqrt{2}}\Delta_x S$$

$$\Sigma_z = \frac{\vec{\Omega}_{1z} + \vec{\Omega}_{2z}}{2}$$

$$\Delta_z^2 = \frac{\left(|\vec{\Omega}_1|^2 - |\vec{\Omega}_2|^2\right)^2}{4|\vec{\Omega}_1 + \vec{\Omega}_2|^2}$$

In a preferential coordinate system T_0 *is an eigenstate of a soft pair* $|\vec{\Omega}_1| = |\vec{\Omega}_2|$

Eigenvalues: $\lambda_1 = -\lambda_2$ ***and*** $\lambda_3 = -\lambda_4$

$$\lambda_1^2 = \left(\frac{|\vec{\Omega}_1| + |\vec{\Omega}_2|}{2} \right)^2 \qquad \lambda_3^2 = \left(\frac{|\vec{\Omega}_1| - |\vec{\Omega}_2|}{2} \right)^2$$

Spin-dependent recombination turns a pair into interacting

With recombination from S ***the dynamics of the pair is governed by***

$$i\frac{d\rho}{dt} = [\hat{H}, \rho] - \frac{i}{2\tau}\{\rho, |S\rangle\langle S|\}$$

The 16 eigenvalues of the matrix equation can be cast in the form $\lambda_i - \lambda_j^*$

where λ_i ***satisfy the equation***

$$\lambda_i\left(\lambda_i + \frac{i}{\tau}\right)\left(\lambda_i^2 - \Sigma_z^2\right) - \lambda_i^2\left(\Delta_z^2 + \Delta_x^2\right) + \Delta_z^2\Sigma_z^2 = 0$$

$$\Sigma_z^2 = \frac{|\vec{\Omega}_1 + \vec{\Omega}_2|^2}{4} \qquad \Delta_z^2 = \frac{\left(|\vec{\Omega}_1|^2 - |\vec{\Omega}_2|^2\right)^2}{4|\vec{\Omega}_1 + \vec{\Omega}_2|^2} \qquad \Delta_x^2 = \frac{|\vec{\Omega}_1 \times \vec{\Omega}_2|^2}{|\vec{\Omega}_1 + \vec{\Omega}_2|^2}$$

Slow recombination: $\frac{1}{\tau} << |\vec{\Omega}_1|, |\vec{\Omega}_2|$

All the modes of "general type" decay slowly

Solving perturbatively $\lambda_i = \pm\left(\frac{|\vec{\Omega}_1| \pm |\vec{\Omega}_2|}{2}\right) + \delta\lambda_i$

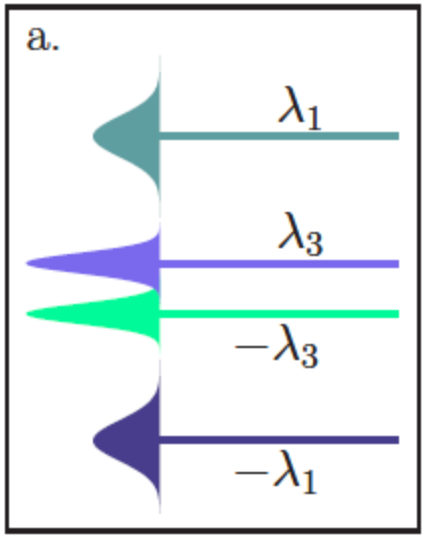

$$\delta\lambda_i = -\frac{i}{2\tau}\frac{\left(\lambda_i^2 - \Sigma_z^2\right)}{2\lambda_i^2 - \left(\Sigma_z^2 + \Delta_z^2 + \Delta_x^2\right)}$$

$$\delta\lambda_{1,2} = -\frac{i}{4\tau}\left(1 - \frac{\vec{\Omega}_1 \cdot \vec{\Omega}_2}{|\vec{\Omega}_1||\vec{\Omega}_2|}\right)$$

$$\lambda_{3,4} = -\frac{i}{4\tau}\left(1 + \frac{\vec{\Omega}_1 \cdot \vec{\Omega}_2}{|\vec{\Omega}_1||\vec{\Omega}_2|}\right)$$

Anomalously long decay times when $\vec{\Omega}_1$ *and* $\vec{\Omega}_2$ *are parallel or antiparallel*

Note that $\frac{\delta\lambda_{3,4}}{\lambda_{3,4}} \sim \frac{1}{b_0\tau}$ *both in low and in high fields*

Slow recombination in soft pairs

$$\lambda_1 = \frac{|\vec{\Omega}_1| + |\vec{\Omega}_2|}{2} >> \frac{1}{\tau}$$ *but* $$\lambda_3 = \frac{|\vec{\Omega}_1| - |\vec{\Omega}_2|}{2} \le \frac{1}{\tau}$$

Only λ_3, λ_4 *should be modified*

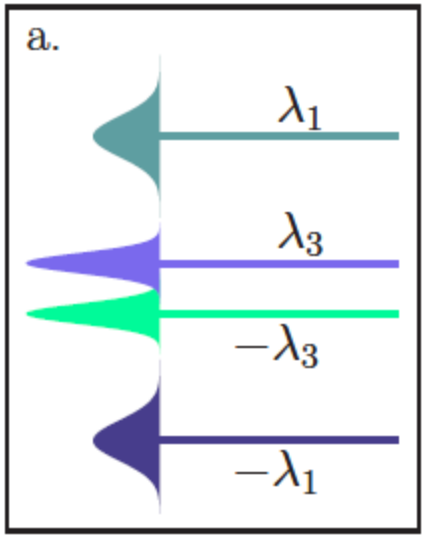

$$\lambda_i\left(\lambda_i + \frac{i}{\tau}\right)\left(\lambda_i^2 - \Sigma_z^2\right) - \lambda_i^2\left(\Delta_z^2 + \Delta_x^2\right) + \Delta_z^2\Sigma_z^2 = 0$$

$$\left(\Sigma_z^2 + \Delta_x^2\right)\lambda^2 + \frac{i}{\tau}\Sigma_z^2\lambda - \Delta_z^2\Sigma_z^2 = 0$$

Critical behavior of splitting

$$\lambda_{3,4} = -\frac{i}{2\tau}\left[\Lambda \pm \sqrt{\Lambda^2 - 4\Lambda\Delta_z^2\tau^2}\right]$$

$$\Delta_z^2 = \frac{\left(|\vec{\Omega}_1|^2 - |\vec{\Omega}_2|^2\right)^2}{4|\vec{\Omega}_1 + \vec{\Omega}_2|^2}$$

small for soft pairs

$$\Lambda = \frac{\Sigma_z^2}{\Sigma_z^2 + \Delta_x^2} = \frac{|\vec{\Omega}_1 + \vec{\Omega}_2|^4}{|\vec{\Omega}_1 + \vec{\Omega}_2|^4 + 4|\vec{\Omega}_1 \times \vec{\Omega}_2|^2}$$

for soft pairs $\Lambda \sim 1$

$$\lambda_{3,4} = -\frac{i}{2\tau}\left[\Lambda \pm \sqrt{\Lambda^2 - 4\Lambda\Delta_z^2\tau^2}\right]$$

$$\Delta_z^2 = \frac{\left(|\vec{\Omega}_1|^2 - |\vec{\Omega}_2|^2\right)^2}{4|\vec{\Omega}_1 + \vec{\Omega}_2|^2}$$

sign "-" describes a long-living mode with lifetime $\sim \left(\Delta_z^2\tau\right)^{-1}$ ***which gets longer with decreasing*** τ

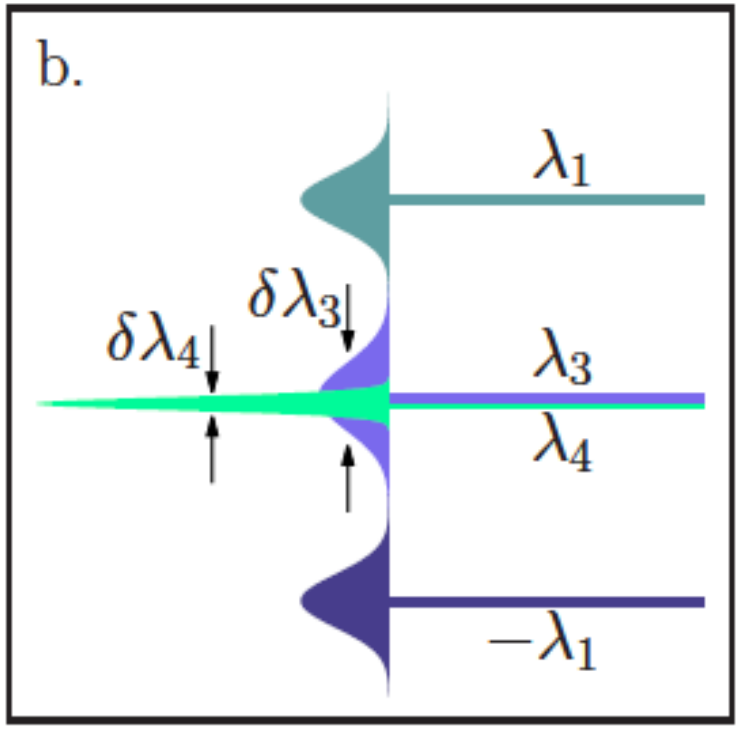

Recombination affects strongly the pair dynamics

PHYSICAL REVIEW VOLUME 93, NUMBER 1 JANUARY 1, 1954

Coherence in Spontaneous Radiation Processes

R. H. DICKE
Palmer Physical Laboratory, Princeton University, Princeton, New Jersey

(Received August 25, 1953)

A simple example will be used to illustrate the inadequacy of this description. Assume that a neutron is placed in a uniform magnetic field in the higher energy of the two spin states. In due course the neutron will spontaneously radiate a photon via a magnetic dipole transition and drop to the lower energy state. The probability of finding the neutron in its upper energy state falls exponentially to zero.[1,2]

If, now, a neutron in its ground state is placed near the first excited neutron (a distance small compared with a radiation wavelength but large compared with a particle wavelength and such that the dipole-dipole interaction is negligible), the radiation process would, according to the above hypothesis of independence, be unaffected. Actually, the radiation process would be strongly affected. The initial transition probability would be the same as before but the probability of finding an excited neutron would fall exponentially to one-half rather than to zero.

PHYSICAL REVIEW B **80**, 033302 (2009)

Quantum transport through nanostructures in the singular-coupling limit

Maximilian G. Schultz and Felix von Oppen

$$H = eV_g(n_\uparrow + n_\downarrow) + \frac{\Omega}{2}(n_\uparrow - n_\downarrow) + Un_\uparrow n_\downarrow + \sum_{k\alpha} \varepsilon_k c^\dagger_{k\alpha} c_{k\alpha} + \sum_{k\alpha\sigma} t_{\alpha\sigma} c^\dagger_{k\alpha} d_\sigma + \text{H.c.}$$

The on-site electronic orbitals are labeled by a pseudospin $\sigma = \uparrow, \downarrow$ and are separated in energy by Ω. This splitting is assumed to be due to symmetry-breaking mechanisms other than electronic tunneling. Double occupation of the system is suppressed by Coulomb repulsion of strength U and both orbitals are coupled to Fermi-gas electrodes $\alpha = L, R$, held in thermal equilibrium at temperature $k_B T$, via lead- and orbital-dependent amplitudes $t_{\alpha\sigma}$.

a straightforward calculation yields for the off-diagonal element of the spectral function

$$\mathcal{A}_{\uparrow\downarrow}(\omega) = \frac{\gamma\left[\left(\omega - \frac{\Omega}{2}\right)\left(\omega + \frac{\Omega}{2}\right) - \frac{\Delta}{4}\right]}{\left|\left(\omega - \frac{\Omega}{2} + \imath\frac{\Gamma_\uparrow}{2}\right)\left(\omega + \frac{\Omega}{2} + \imath\frac{\Gamma_\downarrow}{2}\right) + \frac{\chi^2}{4}\right|^2}$$

The self-energy $\Sigma = \imath\frac{\pi}{\hbar}\nu_0 W^\dagger W$, where $(W)_{\alpha\sigma} := t_{\alpha\sigma}$, gives rise to the broadenings $\Gamma_{\alpha\sigma} := \frac{2\pi}{\hbar}\nu_0 t^2_{\alpha\sigma}$ and $\gamma_\alpha := \frac{2\pi}{\hbar}\nu_0 t_{\alpha\uparrow} t_{\alpha\downarrow}$, with a missing index indicating that it has been summed over;

Rate-equations approach to transport fails for nearly-degenerate levels

the poles: $$\omega = -\frac{i\Gamma}{2} \pm \left(\frac{\Omega^2}{4} - \frac{\Gamma^2}{4}\right)^{1/2}$$

Average recombination time

Needed to calculate the current: I=1/<t>

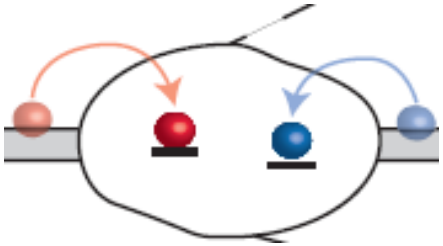

Initial state of a pair is a random superposition of S, T_0, T_-, T_+

What is the average waiting time $\langle t_R \rangle$ *for this state to recombine?*

I. Slow recombination; general pairs $\tau^{-1} << |\vec{\Omega}_1|, |\vec{\Omega}_2|$

With accuracy $\left(|\vec{\Omega}_{1,2}|\,\tau\right)^{-1} << 1$ *the eigenvectors are mutually orthogonal*

$$\langle t_R \rangle = -\frac{1}{8}\sum_j \frac{1}{\mathrm{Im}\lambda_j} = \frac{\tau}{2\left(1-\frac{\vec{\Omega}_1\cdot\vec{\Omega}_2}{|\vec{\Omega}_1||\vec{\Omega}_2|}\right)} + \frac{\tau}{2\left(1+\frac{\vec{\Omega}_1\cdot\vec{\Omega}_2}{|\vec{\Omega}_1||\vec{\Omega}_2|}\right)}$$

II. Slow recombination; soft pairs

$$\Delta_z^2 = \frac{\left(|\vec{\Omega}_1|^2 - |\vec{\Omega}_2|^2\right)^2}{4\,|\vec{\Omega}_1 + \vec{\Omega}_2|^2}$$

$$\lambda_{3,4} = -\frac{i}{2\tau}\left[\Lambda \pm \sqrt{\Lambda^2 - 4\Lambda\Delta_z^2\tau^2}\right]$$

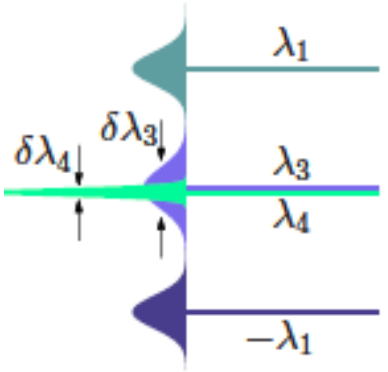

With accuracy $\left(|\vec{\Omega}_{1,2}|\tau\right)^{-1} \ll 1$ *the eigenvectors corresponding to* λ_1 *and* $\lambda_2 = -\lambda_1$ *are mutually orthogonal, and they are both orthogonal to eigenvectors corresponding to* λ_3, λ_4

Eigenvectors corresponding to λ_3, λ_4 *are non-orthogonal for* $\left(|\vec{\Omega}_1| - |\vec{\Omega}_2|\right) \le \tau^{-1}$

Resembles Dyakonov-Perel, but no random walk is involved

$$\langle t_R \rangle = \frac{\tau}{\Lambda} + \frac{1}{4\Delta_z^2\tau} - \frac{1}{\mathrm{Im}\,\lambda_1} - \frac{1}{\mathrm{Im}\,\lambda_2}$$

instead of

$$-\frac{1}{\mathrm{Im}\,\lambda_3} - \frac{1}{\mathrm{Im}\,\lambda_4}$$

exhibits unlimited growth as $\Delta_z \sim \left(|\vec{\Omega}_1| - |\vec{\Omega}_2|\right) \to 0$

Turning to the calculation of current

$$I = \frac{1}{\langle\langle t \rangle\rangle}$$

outside averaging is over the realizations of the hyperfine fields

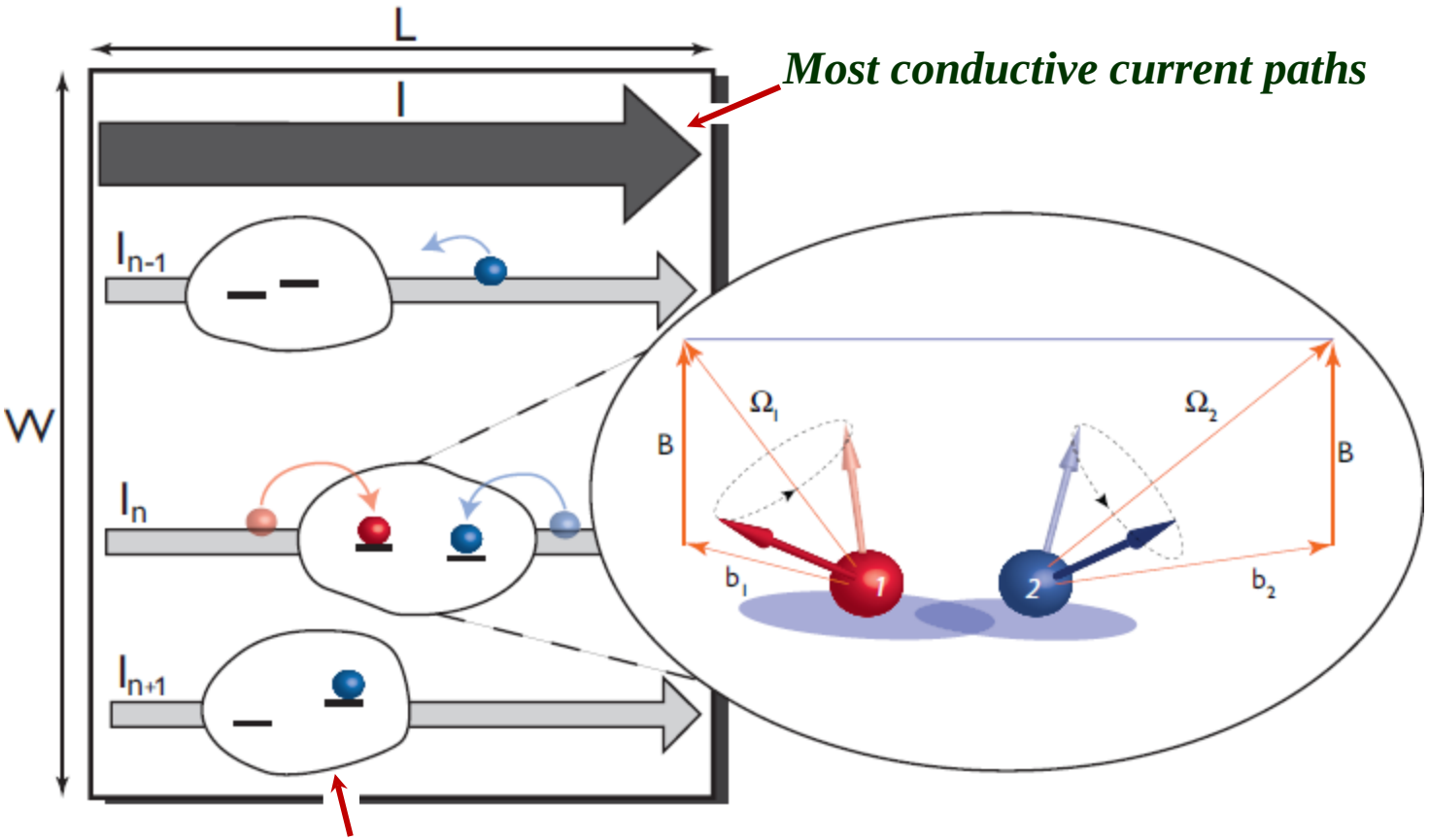

Most conductive current paths

Most resistive junction within a given path

Average duration of the current cycle

$$\bar{t} = \tau_D + \frac{\tau}{1 - \left(\frac{\vec{\Omega}_1 \cdot \vec{\Omega}_2}{|\vec{\Omega}_1 \| \vec{\Omega}_2|} \right)^2}$$

$$I = \frac{1}{\bar{t}} = \frac{1}{\tau_D} - \delta I_t(B)$$

field-dependent part

$$\delta I_t(B) = \frac{\tau}{\tau_D^2} \frac{1}{1 - \left(\frac{\vec{\Omega}_1 \cdot \vec{\Omega}_2}{|\vec{\Omega}_1 \| \vec{\Omega}_2|} \right)^2 + \frac{\tau}{\tau_D}}$$

assembly time of the pair $\tau_D >> \tau$

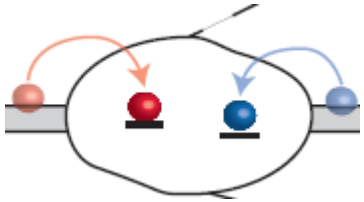

Averaging over distributions of hyperfine fields

$$P\left(\vec{b}_i\right) = \frac{1}{(\pi b_0)^{3/2}} \exp\left(- \frac{|\vec{b}_i|^2}{b_0^2} \right)$$

major change of $\langle \delta I_t(B) \rangle$ *takes place within the domain* $B >> b_0$

$$|\vec{\Omega}_1|^2 |\vec{\Omega}_2|^2 - (\vec{\Omega}_1 \cdot \vec{\Omega}_2)^2 \approx B^2 \left[|\vec{b}_e - \vec{b}_h|^2 - \left(\vec{b}_e \cdot \frac{\vec{B}}{B} - \vec{b}_h \cdot \frac{\vec{B}}{B} \right)^2 \right]$$

expanding with respect to hyperfine fields

$$\langle \delta I_t(B) \rangle = \frac{B^2 \tau}{\tau_D^2} \left\langle \frac{1}{(b_{1x} - b_{2x})^2 + (b_{1y} - b_{2y})^2 + \frac{\tau}{\tau_D} B^2} \right\rangle$$

z-components of the hyperfine field cancel out

$$B_c = \left(\frac{2\tau_D}{\tau} \right)^{1/2} b_0 >> b_0$$

Averaged field-dependent contribution

$$\langle \delta I_t(B) \rangle = \frac{1}{\tau_D} F\left(\frac{B}{B_c}\right) \Leftarrow F(x) = 2x^2 \int_0^\infty du \frac{u}{u^2 + x^2} e^{-u^2} = x^2 e^{x^2} Ei\left(x^2\right)$$

low-field domain

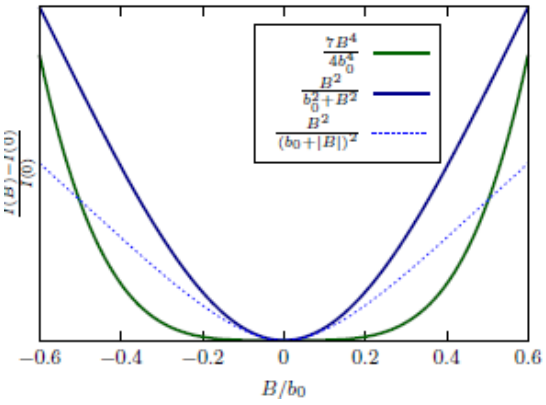

Asymptotic behavior in the domain $b_0 < B << B_c = b_0\left(\frac{2\tau_D}{\tau}\right)^{1/2}$

$$\langle \delta I_t(B) \rangle |_{b_0 < B < B_c} \approx \frac{\tau B^2}{2\tau_D^2 b_0^2} \ln\left(\frac{2\tau_D b_0^2}{\tau B^2}\right)$$

Very low fields: expanding and averaging

$\delta I_t(B)$ *in the domain* $B << b_0$

$$\langle \delta I_t(B) \rangle = \langle \delta I_t(0) \rangle \left(1 + \frac{7B^4}{4b_0^4}\right)$$

$$\langle \delta I_t(0) \rangle = \frac{\tau}{2\tau_D^2} \ln\left(\frac{4\tau_D}{\tau}\right)$$

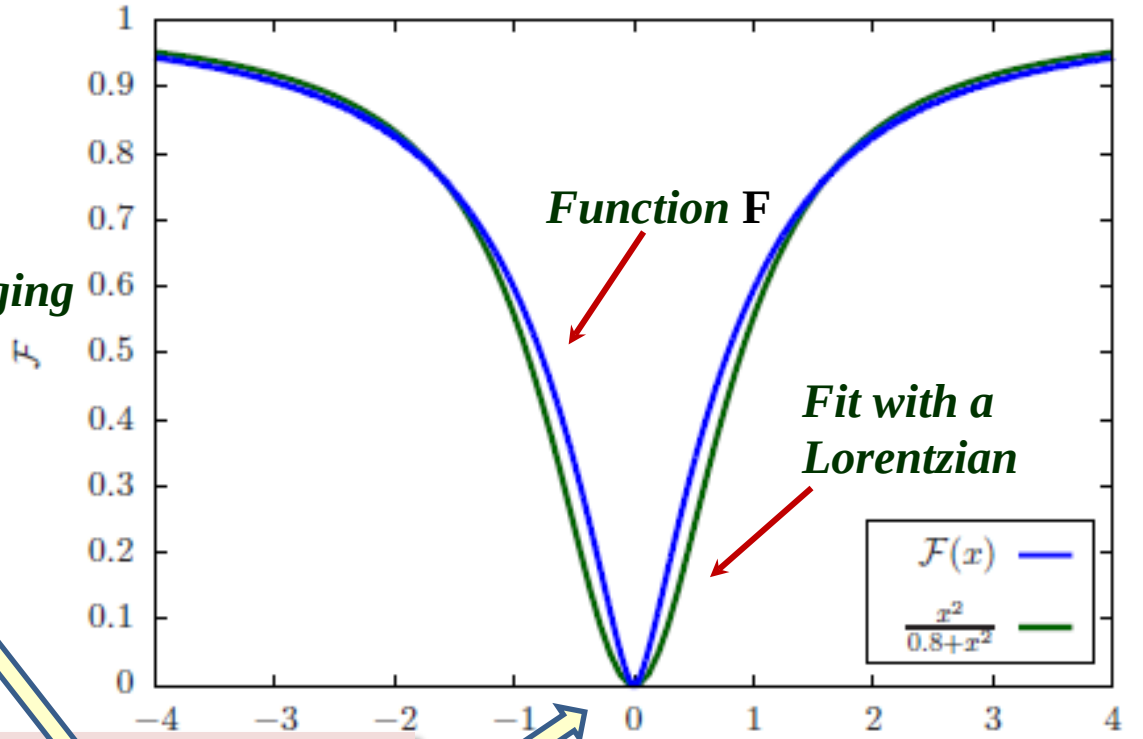

Flat bottom* of *the OMAR lineshape

No feature near zero magnetic field

For $b_1 = b_2$ *magnetic field drops out of the average* $\langle \delta I_s \rangle$

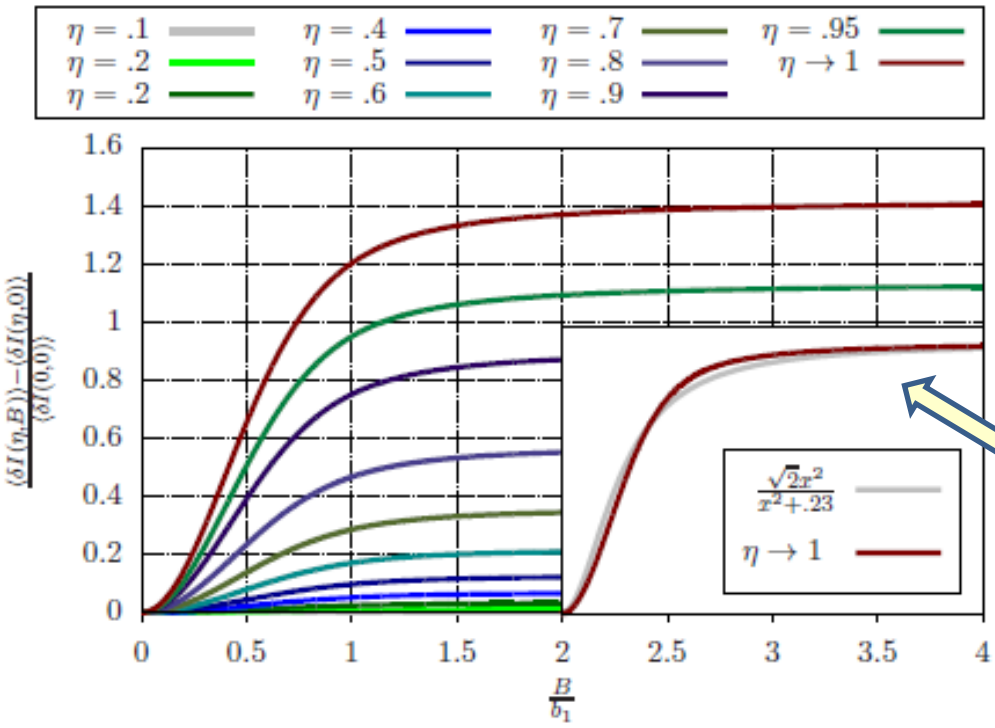

$$\langle \delta I_s(b_1 = b_2) \rangle = \sqrt{\frac{\pi}{2\tau\tau_D^3}}\frac{1}{b_1}$$

comparing to "parallel-antiparallel" correction

$$\langle \delta I_t(0) \rangle = \frac{\tau}{2\tau_D^2}\ln\left(\frac{4\tau_D}{\tau}\right)$$

Fit with a Lorentzian

For a nonzero asymmetry between hyperfine fields:

$$\eta = 1 - \frac{b_2^2}{b_1^2}$$

$$\frac{\langle \delta I_s(\eta, B) \rangle}{\langle \delta I_s(0,0) \rangle} = \sqrt{\frac{2}{2-\eta}} - \left(\frac{\eta}{2-\eta}\right)^2 \left[\frac{1}{\sqrt{2}z} D\left(\frac{2z}{\sqrt{2-\eta}}\right)\right]$$

Dawson function

$$D(x) = e^{-x^2}\int_0^x dt\, e^{t^2}$$

$$z = \frac{B}{b_1}$$

even for $b_1 = b_2$ *an asymmetry in g-factors* $\kappa = \dfrac{g_1 - g_2}{g_1 + g_2}$

leads to a* B*-dependent correction with gaussian shape and opposite sign

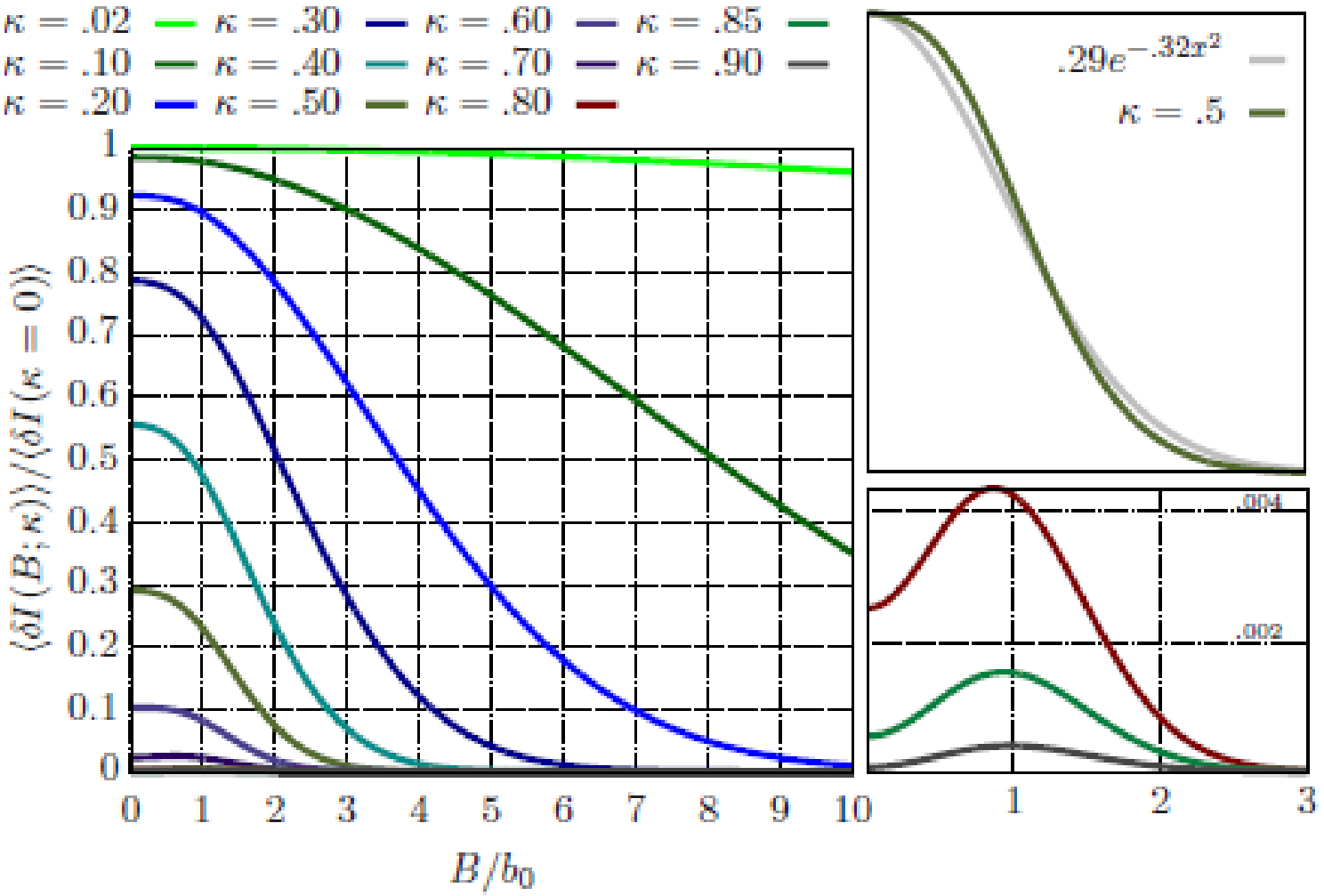

Phase diagram of different regimes

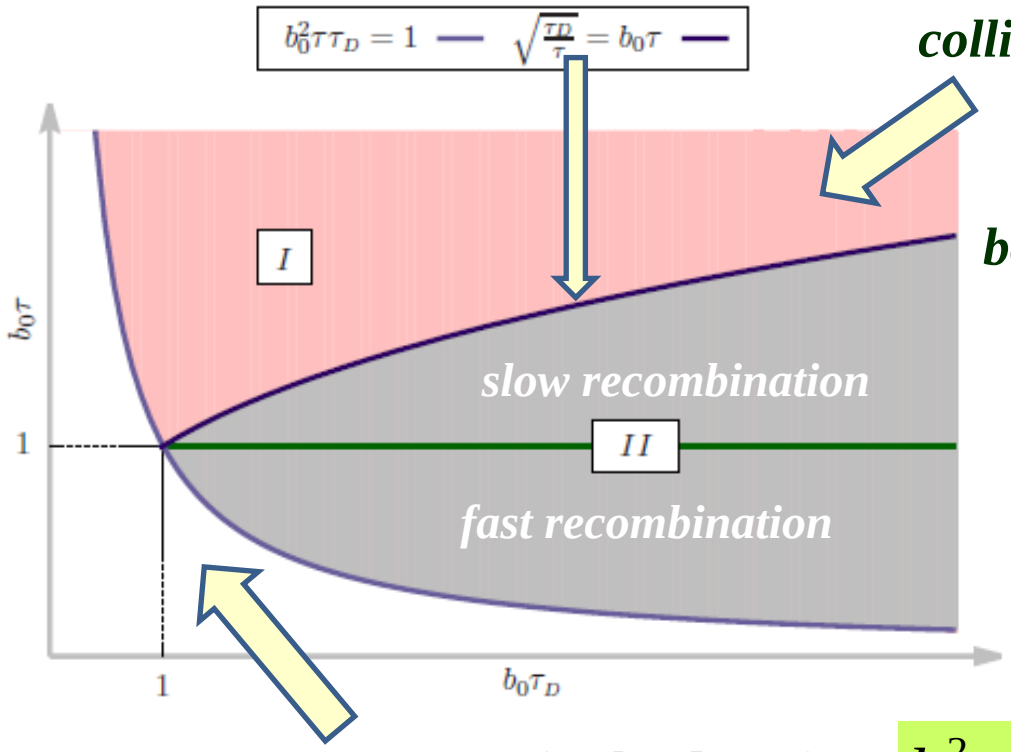

OMAR is dominated by collinear configurations

boundary $\langle \delta I_s \rangle \sim \langle \delta I_t \rangle$

OMAR is dominated by soft pairs

no OMAR in the domain $b_0^2\tau\tau_D < 1$

Related research

Control and Detection of Singlet-Triplet Mixing in a Random Nuclear Field

F. H. L. Koppens,[1]* J. A. Folk,[1]* J. M. Elzerman,[1] R. Hanson,[1]
L. H. Willems van Beveren,[1] I. T. Vink,[1] H. P. Tranitz,[2]
W. Wegscheider,[2] L. P. Kouwenhoven,[1] L. M. K. Vandersypen[1]†

26 AUGUST 2005 VOL 309 SCIENCE

hyperfine field lifts the Pauli blockade

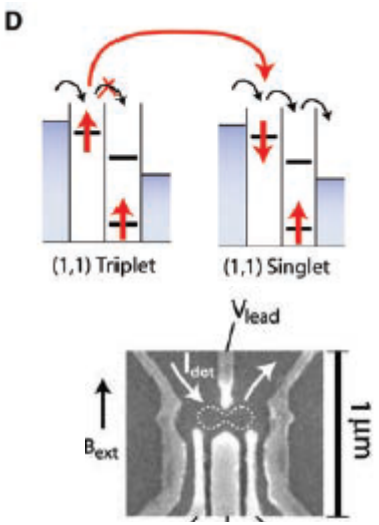

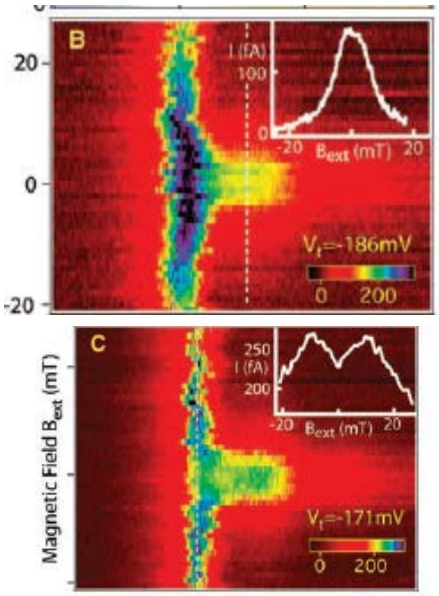

PRL 96, 176804 (2006) PHYSICAL REVIEW LETTERS week ending 5 MAY 2006

Electron Transport in a Double Quantum Dot Governed by a Nuclear Magnetic Field

Oleg N. Jouravlev* and Yuli V. Nazarov
Kavli Institute of NanoScience, Delft University of Technology, Lorentzweg 1, 2628 CJ Delft, The Netherlands
(Received 28 July 2005; published 5 May 2006)

$$\Gamma_R e/I = \left(\frac{t^2}{(B_a^{\parallel})^2} + \frac{F(B_s)}{(B_a^{\perp})^2} \right)$$

parallel -antiparallel

soft pairs

upon averaging

$$I/e = \Gamma_R \frac{t^2 (\boldsymbol{n}_L \times \boldsymbol{n}_R)^2}{8(\Delta^2 + B_s^2)}$$

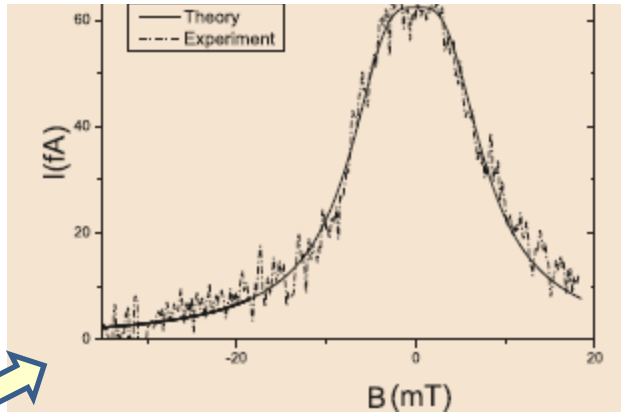

FIG. 4. Fit of experimental data [15] with "flat peak" relation (11) gives $B_N = 4.75$ mT, $\Gamma_{in} = 0.63$ MHz.

Summary

parallel-antiparallel mechanism:

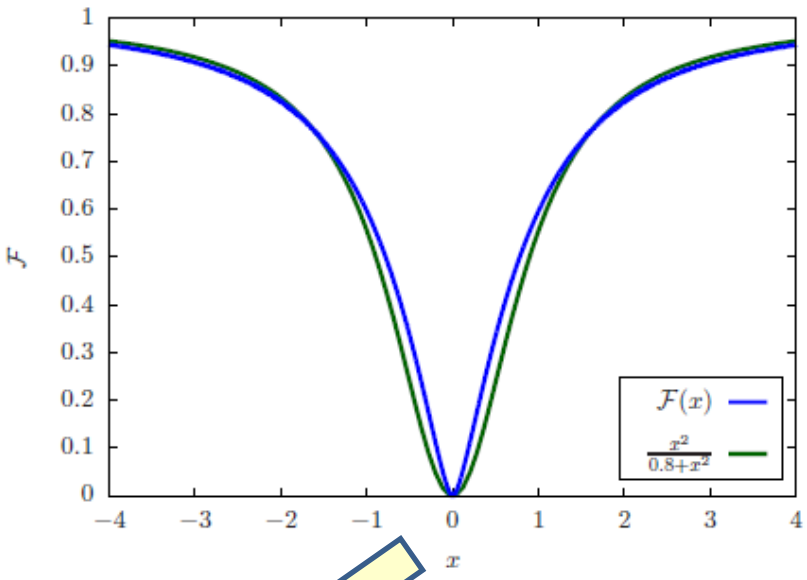

soft pairs with electron-hole asymmetry:

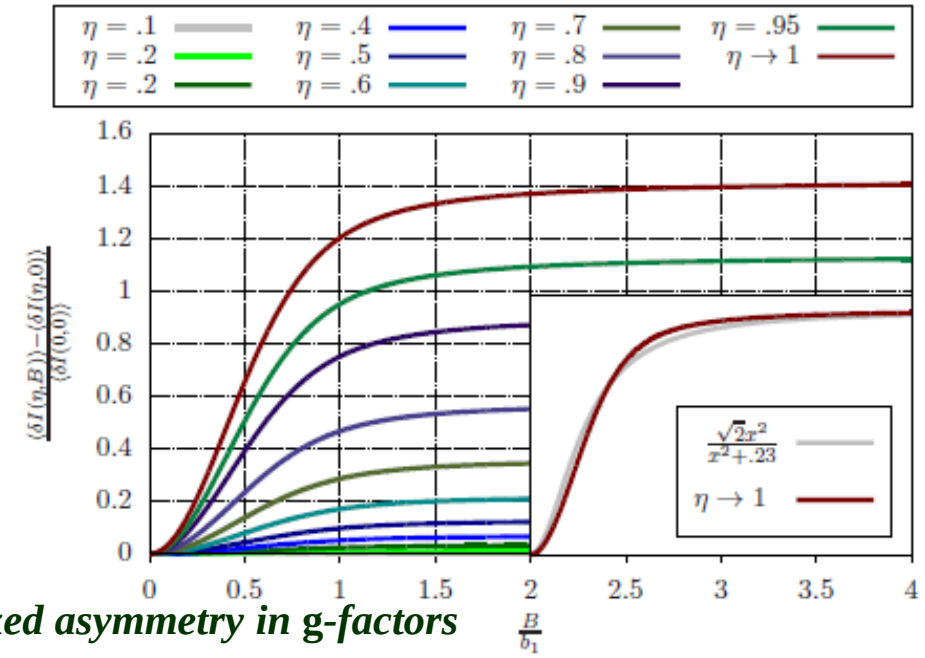

soft pairs with fixed asymmetry in g-factors

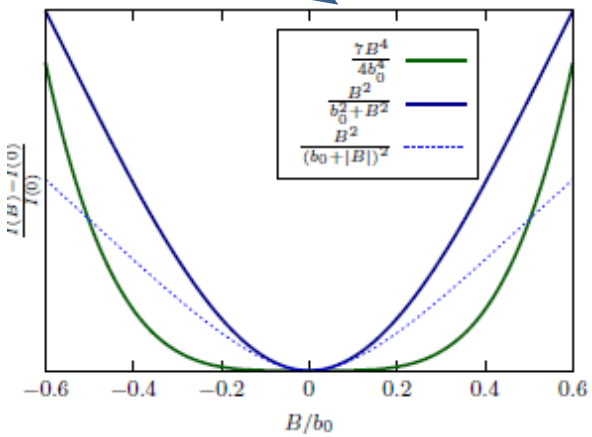

+

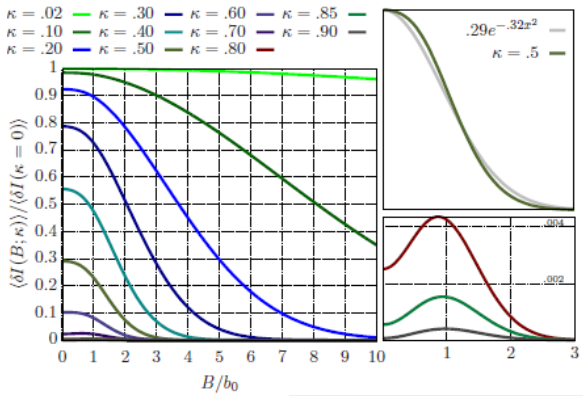

=

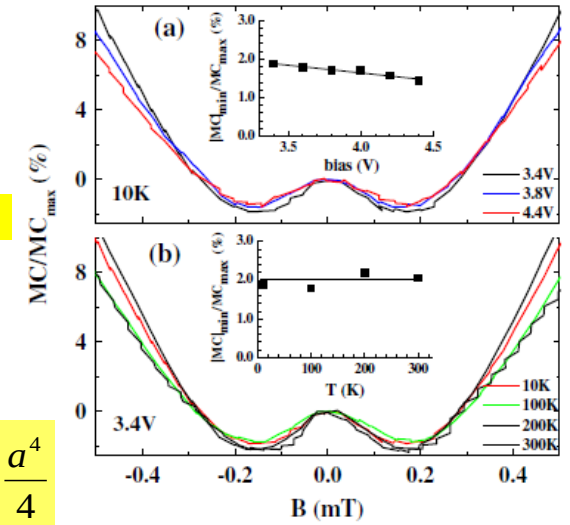

$$x^4 - ax^2 = \left(x^2 - \frac{a}{2}\right)^2 - \frac{a^4}{4}$$